THE MITOTIC SPINDLE MEDIATES INHERITANCE

OF THE GOLGI RIBBON STRUCTURE

APPROVED BY SUPERVISORY COMMITTEE

Joachim Seemann, Ph.D. (Mentor)

Beatriz Fontoura, Ph.D. (Chair)

Helen Yin, Ph.D.

Hongtao Yu, Ph.D.

DEDICATION

To my parents, Yung-Fa and Yu-Chen,

and my mentor Joachim

THE MITOTIC SPINDLE MEDIATES INHERITANCE OF THE GOLGI RIBBON STRUCTURE

by

JEN-HSUAN WEI

DISSERTATION

Presented to the Faculty of the Graduate School of Biomedical Sciences

The University of Texas Southwestern Medical Center at Dallas

In Partial Fulfillment of the Requirements

For the Degree of

DOCTOR OF PHILOSOPHY

The University of Texas Southwestern Medical Center at Dallas

Dallas, Texas

April, 2010

THE MITOTIC SPINDLE MEDIATES INHERITANCE

OF THE GOLGI RIBBON STRUCTURE

JEN-HSUAN WEI, Ph.D.

The University of Texas Southwestern Medical Center at Dallas, 2010

JOACHIM SEEMANN, Ph.D.

The mammalian Golgi ribbon disassembles during mitosis and reforms in both daughter cells after division. Mitotic Golgi membranes concentrate around the spindle poles, suggesting that the spindle may control Golgi partitioning. To test this, cells were induced to divide asymmetrically with the entire spindle segregated into only one daughter cell. A ribbon reforms in the nucleated karyoplasts, whereas the Golgi stacks in the cytoplasts are scattered. However, the scattered Golgi stacks are polarized and transport cargo. Microinjection of Golgi extract together with tubulin or incorporation of spindle materials rescues Golgi ribbon formation. Therefore, the factors required for post-mitotic Golgi ribbon assembly are transferred by the spindle, but the constituents of functional stacks are partitioned independently, suggesting that Golgi inheritance is regulated by two distinct mechanisms.

TABLE OF CONTENTS

PRIOR PUBLICATIONS

1. **Wei JH** and Seemann J (In preparation). Traffic. (Invited review)
2. **Wei JH** and Seemann J (Submitted). Nakiterpiosin targets tubulin and triggers mitotic catastrophe in human cancer cells.
3. **Wei JH** and Seemann J (2009). Induction of asymmetrical cell division to analyze spindle-dependent organelle partitioning using correlative microscopy techniques. Nat Protoc *4*, 1653-1662.
4. **Wei JH** and Seemann J (2009). The mitotic spindle mediates inheritance of the Golgi ribbon structure. J Cell Biol *184*, 391-397.
5. Chakraborty P, Seemann J, Mishra RK, **Wei JH**, Weil L, Nussenzveig DR, Heiber J, Barber GN, Dasso M, Fontoura BM (2009). Vesicular stomatitis virus inhibits mitotic progression and triggers cell death. EMBO Rep *10*, 1154-1160.
6. **Wei JH** and Seemann J (2009). Spindle-dependent partitioning of the Golgi ribbon. Commun Integr Biol *2*, 406-407.
7. **Wei JH** and Seemann J (2009). Mitotic division of the mammalian Golgi apparatus. Semin Cell Dev Biol *20*, 810-816. (Invited review)
8. **Wei JH** and Seemann J (2009). Remodeling of the Golgi structure by ERK signaling. Commun Integr Biol *2*, 35-36.
9. Chakraborty P, Wang Y, **Wei JH**, van Deursen J, Yu H, Malureanu L, Dasso M, Forbes DJ, Levy DE, Seemann J, Fontoura BM (2008). Nucleoporin levels regulate cell cycle progression and phase-specific gene expression. Dev Cell *15*, 657-667.

10. Bisel B, Wang Y, **Wei JH**, Xiang Y, Tang D, Miron-Mendoza M, Yoshimura S, Nakamura N, Seemann J (2008). ERK regulates Golgi and centrosome orientation towards the leading edge through GRASP65. J Cell Biol *182*, 837-843.
11. Bartz R, Sun LP, Bisel B, **Wei JH**, Seemann J (2008). Spatial separation of Golgi and ER during mitosis protects SREBP from unregulated activation. EMBO J *27*, 948-955.
12. Wang Y, **Wei JH**, Bisel B, Tang D, Seemann J (2008). Golgi cisternal unstacking stimulates COPI vesicle budding and protein transport. PLoS One *3*, e1647.
13. **Wei JH**, Chou YF, Ou YH, Yeh YH, Tyan SW, Sun TP, Shen CY, Shieh SY (2005). TTK/hMps1 participates in the regulation of DNA damage checkpoint response by phosphorylating CHK2 on threonine 68. J Biol Chem *280*, 7748-7757.

LIST OF FIGURES

LIST OF TABLES

Chapter One Introduction

Mitotic division of the mammalian Golgi apparatus

Successful cell reproduction requires faithful duplication and proper segregation of cellular contents, including not only the genome but also intracellular organelles. Since the Golgi apparatus is an essential organelle of the secretory pathway, its accurate inheritance is therefore of importance to sustain cellular function. Regulation of Golgi division and its coordination with cell cycle progression involves a series of sequential events that are subject to a precise spatiotemporal control. Here, I summarize the current knowledge about the underlying mechanisms, the molecular players and the biological relevance of this process, particularly in mammalian cells, and discuss the unsolved problems and future perspectives opened by the recent studies.

1. Introduction

1.1 Golgi architecture and function

The Golgi apparatus is a membrane-bound organelle that is essential for protein glycosylation, lipid biosynthesis and secretory trafficking. Despite the functional conservation throughout eukaryotic evolution, the morphology and spatial organization of the Golgi complex vary among different species. In the budding yeast *S. cerevisiae*, for instance, Golgi membranes are organized as single cisternae (Preuss et al., 1992). This is

in contrast to most eukaryotic cells where the cisternae are closely arranged in parallel to form stacks. In protozoa, plants and lower animals, the Golgi stacks are dispersed throughout the cytoplasm (He, 2007). In vertebrates, however, the individual stacks are tethered together by membranous tubular bridges into a single continuous ribbon. The Golgi ribbon normally resides in the perinuclear region and in close proximity to the centrosomes (Ladinsky et al., 1999). In the secretory pathway, the Golgi functions as a trafficking hub that processes newly synthesized proteins from the ER and sorts them to their appropriate destinations. Furthermore, the orientation of the Golgi ribbon is of crucial importance to establish and maintain cellular polarity, since it guides the exocytic traffic towards a specific domain of the plasma membrane (Yadav et al., 2009).

1.2 Organelle inheritance

In principle, cellular organelles can be maintained either by inheritance or by *de novo* assembly (Lowe and Barr, 2007). *De novo* formation refers to the process by which the organelle is generated by its constituents without a copy from the progenitors. By strict definition, a functional organelle can be assembled from the molecular components encoded in the genome and the cellular machinery needed for the assembly process. In this regard, recycling endosomes and peroxisomes have been shown to possess the capacity to form *de novo* (Kim et al., 2006; Sheff et al., 2002). The alternative is to inherit the organelle from the progenitors. Inheritance requires a pre-existing template or seed that serves as a blueprint or building block for the growth and division processes. Template inheritance requires not only the materials that compose the organelle but also

the epigenetic information stored within the organellar structure. These two mechanisms are not mutually exclusive, although in most cases inheritance plays a dominant role over *de novo* assembly. This might reflect the stringent demands for accurate and efficient biogenesis, especially when structural complexity increases along evolution. Therefore, *de novo* assembly can be regarded as a fail-safe design in case inheritance of the template is defective (Shorter and Warren, 2002).

Depending on the copy number of organelles, different strategies can be employed to ensure accurate inheritance (Warren and Wickner, 1996). For example, multi-copy organelles such as mitochondria and peroxisomes can be stochastically distributed between progeny during cell division. In contrast, single-copy organelles need to be doubled prior to cell division either in number (e.g. centrosomes and chromosomes) or in size (e.g. the single Golgi stack in *Toxoplasma*) and later equally split into the nascent daughter cells (He, 2007). Single-copy organelles can also be divided using a modified strategy by which they are first disassembled into multiple subunits and then partitioned into the offspring (e.g. the Golgi ribbon in vertebrates). In any case, the accuracy and efficiency of organelle inheritance are greatly influenced by the number of the partitioning units as well as the strategies taken. In theory, when provided with a sufficient number of units, organelles can be partitioned by a passive, stochastic process without much compromise of accuracy and efficiency. It becomes a challenge, however, when the copy number is low. Instead, an active, ordered segregation mechanism is used, which is often organized by the microtubule-based spindle machinery.

1.3 Overview of mammalian Golgi division

The mammalian Golgi is present as a single continuous ribbon, which must be divided into the two daughter cells during mitosis. Golgi division is achieved in three consecutive steps. First, at the onset of mitosis, the Golgi ribbon is laterally unlinked and then the cisternae unstack, which are further disassembled into tubular and vesicular membranes. Next, concomitant with chromosome segregation, the mitotic Golgi membranes are evenly partitioned into the daughter cells. Finally, upon mitotic exit the membranes fuse and reassemble into a functional Golgi. Accompanied with the disassembly upon mitotic entry, the secretory function of the mammalian Golgi is impaired due to a global inhibition of membrane fusion (Warren, 1993). In contrast, secretion continues throughout plant cell division to deliver membranes to the division plane for cell plate formation (Nebenfuhr et al., 2000). Since mitotic inhibition of membrane fusion is not a common feature of all organisms, it might have evolved as an efficient way to disassemble the mammalian Golgi at the onset of mitosis. Moreover, shutdown of the membrane exchange between different compartments might be an additional secure device to prevent undesired activation of certain biochemical pathways (Bartz and Seemann, 2008).

2. Prior to disassembly: role of Golgi in G2/M transition

The order and dependency of critical events during the cell cycle is enforced by a surveillance mechanism termed checkpoints. In response to unsatisfied checkpoints, signaling cascades are triggered and sustained to delay cell cycle progression. As a consequence, cells are either arrested at a specific stage of the cell cycle for repair or committed to programmed cell death when the errors or damages are too severe to be resolved. These essential modules, including G1/S, intra-S, G2/M and spindle assembly checkpoints, are designated to detect various types of DNA lesions, stalled replication forks, and inappropriate microtubule attachment or tension generated at the kinetochores (Tyson and Novak, 2008). Recently, several groups have suggested a novel non-DNA-associated checkpoint that senses the morphological change of the Golgi in late G2 phase (Rabouille and Kondylis, 2007). As a prelude to mitotic disassembly, the lateral connections between the stacks are severed, which converts the ribbon into individual stacks (Colanzi et al., 2007). While the conventional G2/M checkpoint assures genomic integrity, the Golgi-based checkpoint monitors the structural integrity of the organelle itself and defines another prerequisite for mitotic entry. Kinases (MEK1, ERK2/1c and Plk3), effectors on the Golgi (GRASP65 and GRASP55) and the membrane fission machinery (BARS) have been shown to participate in this process.

Unlinking of the Golgi ribbon depends on the activation of the MEK1/ERK signaling cascade. Inhibition of MEK1 decreases the number of Golgi elements in late G2 phase as well as the mitotic index, suggesting that ribbon unlinking is important to trigger mitotic

entry (Feinstein and Linstedt, 2007). Likewise, a delay in mitotic entry is observed upon downregulation of MEK1 by RNAi. In agreement with the idea, the requirement for MEK1 in mitotic entry can be bypassed either by dispersion of the Golgi structure with brefeldin A (BFA) or by depletion of GRASP65 (Feinstein and Linstedt, 2007). Moreover, ERK1c and Plk3 have been reported to act downstream of MEK1 and contribute to mitotic Golgi fragmentation (Shaul and Seger, 2006; Xie et al., 2004), although the precise stage and the exact mechanism remain to be elucidated.

Two downstream targets of the MEK1/ERK pathway on the Golgi, GRASP65 and GRASP55, possess the ability to modify the Golgi structure as well as to regulate mitotic progression. GRASP65 is a Golgi cisternal stacking factor that holds adjacent cisternae together both *in vitro* and *in vivo* (Barr et al., 1997; Wang et al., 2003; Wang et al., 2008b). Recent investigations have further suggested that GRASP65 can laterally connect stacks into a ribbon (Puthenveedu et al., 2006). Similarly, GRASP55 functions in cisternal stacking as well as lateral linking of stacks (Feinstein and Linstedt, 2007; Shorter et al., 1999). The involvement of GRASP proteins in G2/M transition was first revealed in a functional study showing that antibodies against GRASP65 or a C-terminal mutant of GRASP65 inhibits mitotic Golgi fragmentation in semi-intact cells and reduces the mitotic population of microinjected cells (Sutterlin et al., 2002). Furthermore, when Golgi integrity is disrupted with BFA or nocodazole, these cells traverse through the G2/M boundary. This led to the proposal of a checkpoint that couples compromised Golgi integrity to mitotic entry. Interestingly, expression of a phosphorylation-resistant mutant but not wildtype GRASP65 alleviates the mitotic delay, suggesting that Golgi

integrity and mitotic entry are intimately linked though phosphorylation (Preisinger et al., 2005; Yoshimura et al., 2005). GRASP55 is also regulated by phosphorylation; however, entry into mitosis is instead delayed in cells expressing the phosphorylation-deficient mutant (Duran et al., 2008; Feinstein and Linstedt, 2007).

Mitotic Golgi fragmentation also depends on CtBP/BARS, a bi-functional protein involved in both gene regulation and membrane trafficking (Corda et al., 2006; Nardini et al., 2003). BARS was identified as a key component that induces Golgi fission and promotes mitotic entry. Inhibition of BARS by antibodies, dominant-negative mutants or down-regulation of BARS by antisense oligos prevents both mitotic Golgi fragmentation and entry into mitosis (Hidalgo Carcedo et al., 2004). BARS-dependent Golgi fission occurs in late G2 phase when the Golgi ribbon is converted into isolated stacks via cleavage of interconnecting tubules (Colanzi et al., 2007). However, although BARS knockout in mice is embryonic lethal, the derived mouse embryonic fibroblasts (MEFs) proliferate normally, which contradicts the proposed role of BARS in mitotic entry. Several possibilities have been put forward to explain this discrepancy. First, mechanisms other than BARS-dependent tubulation (e.g. COPI-dependent vesiculation or dynamin-driven cleavage of tubules) might facilitate mitotic Golgi fragmentation (Hidalgo Carcedo et al., 2004). Second, other pathways might compensate for the lack of BARS and therefore override the requirement for BARS in mitotic entry. Indeed, a loss of a normal ribbon organization has been found in BARS knockout MEFs (Colanzi et al., 2007).

In brief, suppression of either the kinase signaling on the Golgi or the membrane fission machinery restricts ribbon unlinking and causes a delay in mitotic entry. However, several questions remain to be answered. First, inhibition of ribbon unlinking in most studies results in a mitotic delay instead of an arrest at the G2/M boundary (Feinstein and Linstedt, 2007; Preisinger et al., 2005). The strength of the checkpoint response seems weak compared to the classical DNA damage checkpoint. In line with this notion, several groups reported that MEK1 activity is neither required for mitotic Golgi fragmentation nor for entry into mitosis (Draviam et al., 2001; Lowe et al., 2000; Lowe et al., 1998; Shinohara et al., 2006). In addition, several key components of the intrinsic G2/M checkpoint have been found on the Golgi, including the Myt1 kinase (Nakajima et al., 2008) and CyclinB2 (Draviam et al., 2001). Analysis of the crosstalk between these two checkpoints should provide further insights into how Golgi integrity influences mitotic entry and progression. Finally, despite the discovery of two modules as key regulators of Golgi fragmentation and mitotic progression, the mechanisms by which they operate remain to be unraveled.

3. Disassembly

Once the cell is committed to mitosis, the microtubule network is rapidly remodeled and the two centrosomes migrate to opposite sides of the nucleus to setup the bipolar spindle. Concomitant with the cytoskeletal rearrangement, the Golgi stacks unlink and distribute with the centrosomes in late G2/early prophase (Shima et al., 1998). In response to elevated Cdk1 activity, the Golgi cisternae then unstack and break down into vesicles and tubules termed mitotic Golgi clusters (MGCs). The disassembled Golgi membranes accumulate around the nascent spindle poles and parts of MGCs continue to shed vesicles that spread throughout the cytoplasm (Lowe et al., 2000). Through unstacking, vesiculation and tubulation, the single interphase Golgi ribbon is thus transformed into numerous small units in preparation for subsequent partitioning (Jesch et al., 2001b).

3.1 Cisternal unstacking

GRASP65 and GRASP55 are essential regulators of Golgi cisternal stacking (Barr et al., 1997; Shorter et al., 1999). GRASP65 forms homo-dimers, which further oligomerize *in trans* (Wang et al., 2003). Since GRASP65 is anchored to the Golgi membrane via an N-terminal myristic acid, oligomerization at two apposing membranes cross-bridges and therefore stacks the cisternae. Upon phosphorylation, GRASP65 oligomerization is disrupted and cisternal stacking is accordingly abolished (Wang et al., 2003). Unstacking increases the membrane surface area accessible for vesicle budding, which speeds up COPI-dependent vesiculation and therefore facilitates the rapid disassembly of the Golgi

at the onset of mitosis (Wang et al., 2008b). Unstacking is triggered by distinct sets of kinases under different physiological conditions. Upon stimulation with mitogens, GRASP65 is phosphorylated by ERK through the MAP kinase pathway (Bisel et al., 2008; Yoshimura et al., 2005). On the other hand, to facilitate Golgi disassembly, both GRASPs are heavily phosphorylated upon mitotic entry. Whereas GRASP65 is the target of Cdk1/CyclinB1 and Plk1 (Lin et al., 2000; Wang et al., 2003), GRASP55 was identified as a substrate of ERK2 in mitosis (Jesch et al., 2001a). Whether GRASP55 is also phosphorylated by Cdk1/CyclinB1 and Plk1 and whether GRASP55 phosphorylation contributes to unstacking remain to be established.

3.2 COPI-dependent vesiculation

To support transport through the Golgi stacks, COPI vesicles bud from one cisterna and fuse with the next cisterna in the stack. The balance between vesicle formation and fusion is tightly regulated to maintain the polarized composition of the Golgi stacks. In mitosis, however, the equilibrium is disturbed and preferentially shifted from membrane fusion towards vesicle budding. Fusion of vesicles with the cisternae is impaired due to inhibition of vesicle tethering. To achieve tethering, the cytosolic factor p115 simultaneously binds to GM130 on the Golgi cisterna and giantin on the COPI vesicle. This brings the two membranes into close proximity (Sonnichsen et al., 1998) and catalyzes membrane fusion (Diao et al., 2008; Shorter et al., 2002). During mitosis, GM130 is phosphorylated by Cdk1, which prevents p115 from binding and thereby inhibits tethering and subsequent vesicle fusion (Lowe et al., 2000). Sustained budding in

the absence of fusion rapidly consumes the cisternae and leads to the mitotic fragmentation of the Golgi. Consistent with this notion, Arf1 is active during mitosis and its activity is required for mitotic Golgi disassembly (Xiang et al., 2007).

3.3 COPI-independent fragmentation

Golgi fragmentation can also proceed in a COPI-independent manner which transforms cisternae into extensive tubular networks (Misteli and Warren, 1995). This pathway is thought to fragment the flattened cisternal core, but its contribution to mitotic Golgi disassembly is not yet clear. Several molecules with the ability to promote tubulation have been implicated in this process, including BARS and Golgi-specific endophilins (Gallop et al., 2005). Remarkably, similar structural changes can be induced by BFA, which relocates Golgi enzymes back to the ER via tubules. It has been suggested that mitotic Golgi breakdown is essentially a phenocopy of BFA treatment that causes inactivation of Arf1 (Altan-Bonnet et al., 2003). In line with this, transiently over-expressed Arf1-GFP loses its Golgi localization in early mitosis. Restricting Arf1 in its active state, either by expression of the constitutively active mutant or by treatment with the protein kinase A inhibitor H89, blocks mitotic Golgi disassembly and causes defects in chromosome segregation and cytokinesis (Altan-Bonnet et al., 2003). Nevertheless, the mechanisms underlying these defects remain largely unknown. In addition, Golgi fragmentation and mitotic progression proceed normally in the cells injected with an active Arf1 mutant, suggesting that Arf1-independent tubulation might play a minor role in mitotic Golgi disassembly under physiological conditions (Xiang et al., 2007).

4. Partitioning

Upon metaphase-anaphase transition, the Golgi fragments are separated into the nascent daughter cells. Two different models have been proposed for Golgi partitioning. In one view, the Golgi is in dynamic equilibrium with the ER and is dependent on the ER for its biogenesis. Based on this concept, it has been proposed that mitotic Golgi membranes are absorbed into and segregated together with the ER (Zaal et al., 1999), a similar mechanism utilized by the nuclear envelope during cell division. The second view suggests that the distinction between the Golgi and the ER persists throughout mitosis and the two compartments are inherited independently (Shorter and Warren, 2002). In accordance, mitotic Golgi membranes concentrate at the spindle poles as well as align along spindle microtubules (Shima et al., 1998). Therefore, the spindle apparatus has been proposed to organize Golgi partitioning. This possibility has been recently tested and the results suggest two levels of regulation acting on Golgi inheritance. Briefly, a spindle-mediated process is required for post-mitotic assembly of the long-range ribbon structure, but secretion-competent Golgi stacks reform in a spindle-independent manner (Wei and Seemann, 2009).

4.1 ER-dependent partitioning

Golgi resident enzymes continuously cycle between the Golgi and the ER during interphase (Cole et al., 1996; Storrie et al., 1998). When anterograde ER-to-Golgi transport is blocked by a dominant negative mutant of Sar1, Golgi enzymes progressively

accumulate in the ER. In early mitosis, COPII vesicle budding from the ER exit sites is also inhibited (Kano et al., 2004). This has led to the concept that the entire Golgi might merge with the ER during mitosis, because Golgi proteins can still return to the ER but become trapped there due to mitotic inhibition of ER export. These conclusions are based on imaging analysis of a GFP-tagged Golgi enzyme and measurements of its subcellular localization, transport rate and diffusional mobility (Zaal et al., 1999). Additionally, a similar ER recycling mechanism was suggested using a temperature-sensitive mutant of VSV-G. When pre-distributed into the Golgi at the onset of mitosis and then shifted back to the non-permissive temperature, VSV-G mutant became misfolded and trapped in the ER (Altan-Bonnet et al., 2006).

4.2 ER-independent partitioning

The alternative mechanism argues that the Golgi is partitioned independently of the ER. During mitosis the Golgi breaks down into clustered or free vesicles that remain isolated from the ER (Axelsson and Warren, 2004; Jesch et al., 2001b). Several approaches have been used to delineate the actual partitioning process. Using fluorescence recovery after photobleaching in combination with pharmacological analysis, Golgi markers have been shown to move in vesicles rather than by lateral diffusion in continuous membranes during mitosis (Axelsson and Warren, 2004). Moreover, an elaborate ER trapping experiment was employed to probe whether the ER and the Golgi merge in mitosis. When co-expressing an FKBP-tagged Golgi enzyme and an ER-retained protein fused to

FRAP, no trapping was found during mitosis in the presence of rapamycin that normally induces a tight association of FKBP with FRAP (Pecot and Malhotra, 2004).

A recent investigation of endogenous SREBP and ATF6 has emphasized the physiological relevance in maintaining the boundaries between the Golgi and the ER during mitosis (Bartz et al., 2008). SREBP and ATF6 are membrane-bound transcription factors that reside as silent precursors in the ER. Upon specific activation signals (low cholesterol for SREBP and ER stress for ATF6), the precursors are transported to the Golgi where they are cleaved by the Golgi-resident proteases S1P and S2P. Cleavage releases the mature forms of SREBP and ATF6 from the membrane, which enter the nucleus to allow gene expression. Silence of these transcription factors critically relies on distinct boundaries between the ER and the Golgi, since the presence of the proteases and substrates in the same compartment is sufficient for activation even in the absence of the activation signals (DeBose-Boyd et al., 1999). At the end of mitosis, no cleavage of SREBP or ATF6 is detected, indicating that the Golgi remains separated from the ER. Thus, tight constraint of the Golgi/ER boundary during cell division prevents unregulated activation of the SREBP and ATF6 pathways (Bartz and Seemann, 2008; Bartz et al., 2008).

4.3 Spindle-dependent inheritance of the Golgi ribbon

In support for the ER-independent partitioning model, mitotic Golgi clusters were found to accumulate around the spindle poles (Shima et al., 1998; Wei and Seemann, 2009),

while the ER was excluded from the spindle area (Jesch et al., 2001b). Detailed dynamic analysis suggested that MGC may serve as the partitioning unit during cell division (Shima et al., 1997). Furthermore, the observed accuracy of Golgi inheritance is higher than expected for a stochastic process, implying an active, ordered partitioning mechanism is involved. In this scenario, the spindle has been proposed as the machinery responsible for partitioning (Shima et al., 1998). To test this, cells were induced to divide asymmetrically with the entire spindle segregated into only one of the daughter cells (Wei and Seemann, 2009). Intriguingly, polarized Golgi stacks reformed in both daughter cells that are functional in secretion. However, the stacks in the cell that received the spindle are interconnected into a continuous ribbon. In contrast, the stacks in the spindle-deprived cell are scattered throughout the cytoplasm. The ribbon can be restored by incorporation of parts of the spindle or when provided with Golgi protein extract, suggesting that specific spindle-associated ribbon determinants are segregated together with the spindle. In sum, the Golgi is inherited by two mechanisms, spindle-dependent partitioning of ribbon factors and spindle-independent inheritance of functional stacks (Wei and Seemann, 2009). The identity of ribbon factors and the underlying mechanisms remain to be defined.

5. Reassembly

The entire Golgi disassembly-reassembly cycle can be reconstituted with purified proteins and rat liver Golgi membranes (Tang et al., 2008). Mitotic disassembly requires Cdk1/CyclinB1 and Plk1 to induce cisternal unstacking, and coatomer and Arf1, the machinery needed for COPI vesicle budding. Golgi reassembly is essentially a reversal of the disassembly process involving membrane fusion and cisternal restacking. Fusion of Golgi membranes into cisternae requires two AAA ATPases, NSF and p97/VCP, which act through two different pathways (Rabouille et al., 1995a). Upon regrowth, cisternae are first aligned by p115 and then stacked by GRASP65 (Shorter and Warren, 1999).

5.1 Cisternal regrowth

Since NSF is a general requirement for most membrane fusion, it is not surprising that the NSF-dependent fusion machinery is essential for Golgi reassembly. Substitution of interphase cytosol with purified NSF, α-SNAP, γ-SNAP and p115 yields stacked cisternae although relatively short in length (Rabouille et al., 1995a). However, the ATPase activity of NSF is dispensable for reassembly (Muller et al., 1999). A possible explanation is that the disengagement of SNAREs by NSF might have occurred during disassembly. Nevertheless, NSF is still needed, indicating that a second NSF activity other than ATP hydrolysis is required. Remarkably, while ATP hydrolysis is not important, the presence of ATP is an absolute requirement (Muller et al., 1999). Another main player in NSF-dependent pathway is p115. Prior to the SNARE-catalyzed fusion

event, p115 tethers vesicles to cisternae via the ternary complex GM130-p115-giantin. In addition, p115 harbors a SNARE-motif related domain that directly binds to the t-SNARE syntaxin-5 and stimulates SNARE complex formation, suggesting an additional role in vesicle docking (Shorter and Warren, 1999).

The second pathway for Golgi cisternal regrowth depends on p97 and its adaptor p47 (Meyer, 2005). p97/p47-dependent fusion generates single, long cisternae, while the NSF pathway fuses membranes into much shorter but stacked cisternae. Golgi reassembly can be fully reconstituted using the components of the two pathways (NSF, α/γ-SNAP, p115, p97 and p47) together with PP2A (Tang et al., 2008). p97 may facilitate Golgi reassembly via two mechanisms. First, based on shared similarities to NSF, p97 is thought to induce membrane fusion through SNAREs. While NSF regulates heterotypic fusion via GOS-28/syntaxin-5, p97 promotes homotypic fusion that requires syntaxin-5 but not GOS-28 (Rabouille et al., 1998). In the latter case, the cofactor p47 is critical since it directs the binding of p97 to syntaxin-5. Another cofactor for p97 is p37, which requires p115 and GOS15 instead of syntaxin-5 (Uchiyama et al., 2006). Second, p97 can either unfold proteins or extract substrates from the existing environment. This remodeling activity often involves the binding of p97 to ubiquitylated substrates via a distinct set of adaptors (Meyer, 2005). Indeed, p47, the adaptor required for p97-dependent Golgi reassembly, contains a UBA (ubiquitin-associated) domain that binds ubiquitin and recruits p97 preferentially to mono-ubiquitylated substrates (Meyer et al., 2002). While p47 is phosphorylated and inactivated by Cdk1 during disassembly (Uchiyama et al., 2003), a yet-to-be-identified substrate(s) on the Golgi is subject to

ubiquitination. In addition, the deubiquitinating enzyme VCIP135 transiently complexes with p97-p47 and is involved in p97/p47-mediated Golgi regrowth (Wang et al., 2004). Therefore, the ubiquitination-deubiquitination cycle somehow guides the entire disassembly-reassembly process in which ubiquitin might be utilized as a signal to label the status of the Golgi. The exact nature of the ubiquitylated substrate(s) on the Golgi and the underlying mechanism warrants further investigation.

5.2 Cisternal restacking

p115 initiates restacking of cisternae by binding to GM130 and giantin on opposite cisternae (Sonnichsen et al., 1998). This occurs in an early phase of reassembly and is relatively transient, since disruption of the p115 tethers in the later stage does not influence stacking (Shorter and Warren, 1999). Furthermore, p115-mediated restacking is enhanced by GTPγS and is sensitive to microcystin, a selective inhibitor of PP2A (Rabouille et al., 1995b). PP2A counteracts Cdk1 by removing the phosphorylation of GM130 at the end of mitosis, which allows its re-association with p115 and therefore facilitates cisternal stacking. On the other hand, the formation of the ternary complex GM130-p115-giantin is regulated by the small GTPase Rab1, which might explain the stimulation of stacking by GTPγS (Beard et al., 2005). Upon initial alignment of the cisternae by p115, the link between the cisternae is strengthened by the stacking factor GRASP65. GRASP65 was isolated as a Golgi reassembly stacking protein based on its sensitivity to the thiol-alkylating agent N-ethylmaleimide (NEM) in the reassembly reaction (Barr et al., 1997). Moreover, antibodies against GRASP65 or recombinant

GRASP65 suppress restacking both *in vitro* and in post-mitotic cells (Shorter et al., 1999; Wang et al., 2008b). Recently, it has been shown that GRASP65 is also dephosphorylated by PP2A, which resumes its *trans*-oligomerization and thereby links cisternae into stacks (Tang et al., 2008).

6. Post-reassembly: role of Golgi in cytokinesis

During telophase, the Golgi reassembles into two distinct ribbons on the opposite sides of the nucleus in each prospective daughter cell (Gaietta et al., 2006; Seemann et al., 2002). The larger Golgi is located next to the centrosome in the perinuclear area, while the smaller Golgi is positioned next to the midbody and flanking the intracellular bridge between the two daughter cells. At the later stage of cytokinesis, the smaller Golgi migrates to the opposite side of the nucleus and merges with the larger Golgi into a continuous ribbon (Gaietta et al., 2006). It remains unclear why the Golgi is present in two separate pools and whether the rejoining of these two Golgi pools is functionally important. However, the movement of the smaller Golgi in the two daughter cells is asynchronous (Gaietta et al., 2006), which is reminiscent of the asymmetric behavior of mother centrioles during animal cytokinesis (Piel et al., 2001). As a result of centrosome splitting in post-anaphase, the mother centriole separates from the daughter centriole in only one of the daughter cells, transiently repositions to the intracellular bridge and then migrates back to the cell center (Piel et al., 2001). The remarkable similarities between centriole and Golgi movements raise the possibility that the Golgi may participate in the terminal, asymmetric abscission step. In agreement with the idea, Golgi-derived vesicles are primarily delivered from one of the daughter cells into the midbody region where they fuse with and seal off the plasma membrane. This process requires the centrosomal and midbody protein centriolin that anchors the exocyst and SNAREs to the abscission site (Gromley et al., 2005). However, symmetric membrane delivery from two daughter cells into the cleavage furrow has also been reported (Goss and Toomre, 2008). In this context,

both the Golgi and the Rab11-positive recycling endosomes have been implicated as the contributors of deposited membranes (Riggs et al., 2003).

The requirement for Golgi-derived membranes in cytokinesis has been extensively shown in plants. During plant cell division, post-Golgi secretory vesicles are recruited to the cell center by an equatorial array of microtubules known as the phragmoplast (Jurgens, 2005). Notably, in plants Golgi-derived membranes gradually fuse and expand from the cell center towards the cortex, until they eventually merge with the plasma membrane and physically separate the two daughter cells. In contrast, animal cytokinesis is primarily driven by the actin-myosin contractile ring, which not only serves as a scaffold for various key regulators of cytokinesis, but also applies the actual force that drives the plasma membrane to invaginate (Glotzer, 2001). Despite the prevailing role of mechanical constriction, membrane addition is a key factor for animal cytokinesis. The direct involvement of the Golgi as a membrane source has been demonstrated in lower organisms. In *Drosophila*, for example, several Golgi-associated proteins including COG5, syntaxin-5 and the golgin Lava Lamp are required for cytokinesis during spermatogenesis and embryo cellularization (Farkas et al., 2003; Sisson et al., 2000; Xu et al., 2002). In support of the notion, BFA induces cellularization defects in *Drosophila* embryos as well as precludes the first zygotic division in *C. elegans* (Sisson et al., 2000; Skop et al., 2001). However, certain vertebrate tissue culture cells can divide in the presence of BFA (Seemann et al., 2002). Interestingly, although cytokinesis during mouse oocyte maturation proceeds in the presence of BFA, asymmetric spindle

positioning and thus polar body formation are abolished (Wang et al., 2008a). The exact role of the Golgi in this process still awaits elucidation.

In addition to supplying vesicles into the cleavage furrow, the Golgi may actively regulate cytokinesis through a different mechanism. Key cytokinesis modulators are associated with the Golgi in interphase but become released during mitotic disassembly. This is best exemplified in the case of the Golgi peripheral protein Nir2. In mitosis, Nir2 dissociates from Golgi membranes upon Cdk1 phosphorylation and relocates to the cleavage furrow and midbody. It has been proposed that Nir2 exerts its effects on cytokinesis via binding to Plk1 and the GTPase RhoA (Litvak et al., 2004). It will be interesting to determine whether the Golgi functions as a reservoir for mitotic regulators in other biological processes. In light of this, a Golgi-associated protein ACBD3 is released during mitosis and interacts with the signaling protein Numb to specify cell fate, further emphasizing an intricate coordination between cell fate determination and cell cycle progression (Zhou et al., 2007).

7. Outlook

Golgi disassembly and reassembly is highly coordinated with mitotic progression and requires elaborate cooperation of a variety of cellular components. Accumulating evidence also suggests that Golgi division in turn profoundly influences mitosis itself. Therefore, the future challenge is to identify these involved molecular players and to gain more insights into mechanistic details. In addition, it will be of great interest to investigate whether this process is altered in other development stages or under pathological conditions such as cancer or other diseases.

Chapter Two Methodology

Induction of asymmetrical cell division to analyze spindle-dependent organelle partitioning using correlative microscopy techniques

This protocol describes an assay for induction of asymmetrical cell division where the entire spindle is segregated into only one of the daughter cells. The procedure consists of four stages: (i) generation of asymmetrical monoasters by arresting cells in early mitosis with a kinesin Eg5 inhibitor; (ii) induction of cell division by microinjection of recombinant Mad1 protein or by addition of a Cdk1 inhibitor; (iii) monitoring the division process by phase-contrast time-lapse microscopy; and (iv) processing for correlative immunofluorescence or correlative electron microscopy. This approach can be applied to determine the requirement for the mitotic spindle in organelle partitioning as well as to investigate the role of the monopolar spindle in cytokinesis. Moreover, the generated nucleus-lacking cytoplast provides an ideal environment to test the feasibility and activity of biological processes in the absence of genomic influence. The protocol takes 2-4 days to complete.

1. Introduction

To maintain proper cellular function over generations, not only the genetic material but also intracellular organelles must be inherited from progenitors during cell division. Faithful segregation of chromosomes requires the mitotic spindle, an elaborate microtubule-based machine that captures and separates the sister chromatids into the

nascent daughter cells (Murray and Szostak, 1985). Although chromosome segregation has been extensively studied, the mechanisms of organelle partitioning, for example, of the Golgi apparatus, are far less understood. To facilitate partitioning, the Golgi complex in vertebrate cells rapidly disassembles upon mitotic entry into numerous vesicular and tubular membranes (Lowe and Barr, 2007; Pecot and Malhotra, 2004). Interestingly, these mitotic Golgi membranes accumulate in the vicinity of the spindle poles, suggesting that the mitotic spindle might also play a role in Golgi inheritance (Jokitalo et al., 2001; Seemann et al., 2002; Shima et al., 1998). Whether the spindle indeed partitions the Golgi and other cellular organelles was so far difficult to dissect since interfering with spindle dynamics often causes mitotic arrest and thus aborts the division process. To address these issues, I recently established a system where cytokinesis is uncoupled from and proceeds without chromosome segregation (Wei and Seemann, 2009). More specifically, cells are induced to divide asymmetrically with the entire spindle segregated into only one of the daughter cells, thus allowing the assessment of the requirement for the spindle in Golgi partitioning.

To evaluate whether the spindle is essential for Golgi inheritance, I induce asymmetrical cell division, which generates one daughter cell receiving the entire spindle (karyoplast) and another without it (cytoplast) (Figure 1a). I follow individual nascent pairs of the karyoplast and the cytoplast throughout the asymmetrical division process by phase-contrast time-lapse microscopy. Using correlative immunofluorescence and correlative electron microcopy, I then further examine whether Golgi membranes are present in the

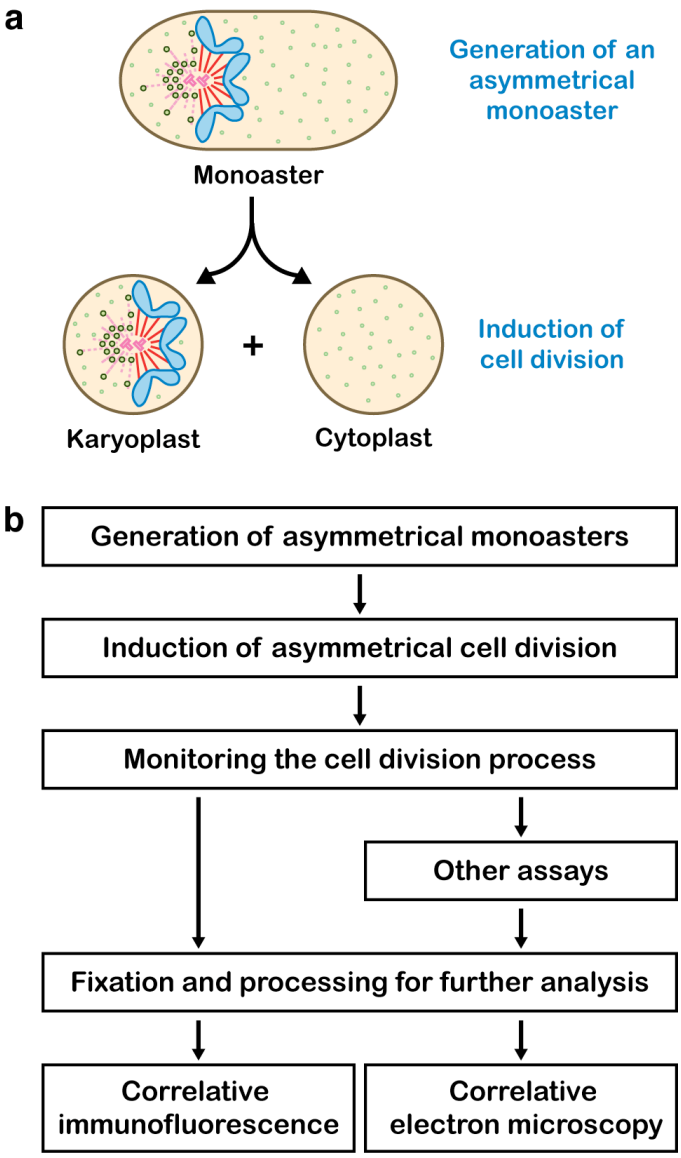

Figure 1. A schematic overview of induction of asymmetrical cell division. (a) Experimental design. Cells are first arrested in mitosis with a kinesin Eg5 inhibitor to generate monoasters. Subsequently the cells are induced to divide asymmetrically into a karyoplast that receives the entire spindle and a cytoplast that lacks the spindle. (b) A flow chart of the protocol. The four major stages of the protocol are: generation of asymmetrical monoasters, induction of asymmetrical cell division, monitoring the division process by phase-contrast time-lapse microscopy, and processing for correlative immunofluorescence or correlative electron microscopy.

spindle-deprived cytoplast and, if any, whether they are structurally altered. Additionally, in combination with microinjection techniques, other assays can be performed such as transport of newly synthesized transmembrane proteins along the secretory pathway to test the functionality of the Golgi membranes in the divided cells (Figure 1b).

1.1 Applications of the method

This approach to induce asymmetrical cell division can be applied to several fundamental questions in cell biology. Given the initial design purpose, this protocol can be used to dissect the requirement for the mitotic spindle in organelle partitioning. In this context, I recently showed that the inheritance of the higher-ordered Golgi structure, termed the Golgi ribbon, requires the mitotic spindle (Wei and Seemann, 2009). However, the basic secretion-competent Golgi stacks are partitioned in a spindle-independent fashion. In addition, this approach has been utilized to improve the mechanistic understanding of mitosis. Asymmetrical division induced by Eg5 inhibition followed by Mad1 microinjection, for instance, demonstrates that the bipolarity of the spindle is not required to determine the position of the cell division plane (Canman et al., 2003). On the other hand, successful induction of monopolar cytokinesis by Cdk1 inhibitors shows that Cdk1 inactivation is sufficient to trigger a signaling pathway leading to cytokinesis (Niiya et al., 2005). Similarly, this approach has been employed to explore the crosstalk between the cell cortex, cytoskeletal components and signaling molecules in furrow specification (Hu et al., 2008). Furthermore, the cytoplast generated by this protocol creates a unique environment where chromosomal material is absent. It can be used to evaluate the

feasibility and activity of a particular biological process in the absence of genomic influence. In light of this, I recently reported that the nucleus-lacking cytoplast possesses the ability to synthesize proteins and to transport cargo from the ER through the secretory pathway to the plasma membrane (Wei and Seemann, 2009).

In addition to the above-described applications, correlative immunofluorescence and correlative electron microscopy described here can be broadly applied to a range of studies that require a detailed localization analysis or an ultrastructural investigation at the single-cell level. The methodology will be particularly useful when only a specific intracellular structure or a distinct phenotype within a large cell population is of interest. However, since our approach is optimized to obtain accurate and detailed morphological information of individual cells, it is less suitable to analyze global changes in a large cell population.

1.2 Experimental Design

1.2.1 PtK_1 cells

In this protocol I induce asymmetrical cell division in PtK_1 cells, a mammalian cell line derived from the kidney of a normal female rat kangaroo. F-12 culture medium is recommended for optimal growth of the cells and to minimize vacuole formation caused by DMEM. The reasons for choosing PtK_1 cells are based on several unique features. First, PtK_1 cells provide a high ratio of asymmetrical monoasters generated by Eg5 inhibition. Compared to other cell lines such as HeLa, Vero, LLC-PK1 and NRK, PtK_1

cells stay relatively flat and only round up slightly during mitosis. Accordingly, spatial restriction in these mitotic cells confines the induced monoasters at one side of the cell. Preservation of the polarized spindle localization is essential since loss of asymmetrical positioning of monoasters often results in flattened cells that return to interphase without division. The efficiency of generating asymmetrical monoasters highly depends on the attachment of the mitotic cells to the glass surface and the contacts with the neighboring cells. The attachment can be improved by growing the culture to full confluency on coverslips coated with Alcian blue or other materials such as collagen or poly-lysine. Second, the chromosome movement of PtK_1 cells can be readily visualized by phase-contrast time-lapse microscopy because of their small number of large chromosomes, relatively large cell size and flat morphology during mitosis (Stout et al., 2006). This greatly simplifies the identification of the division stages. Third, in the case of Golgi division, I observe the most pronounced accumulation of mitotic Golgi membranes around the spindle poles in PtK_1 cells (Jokitalo et al., 2001; Shima et al., 1998). These advantages make them most suitable for the protocol developed here. However, asymmetrical cell division is not limited to PtK_1 cells. Recent studies have reported the formation of asymmetrical monoasters in other species and cell types such as HeLa cells (Hu et al., 2008).

1.2.2 Generation of monoasters

The first step of asymmetrical cell division is to generate monoasters by treatment with monastrol (Mayer et al., 1999), S-trityl-L-cysteine (Skoufias et al., 2006) (Table 1), or other inhibitors of the mitotic kinesin Eg5. Inhibition of the kinesin Eg5 blocks centrosome separation in prophase, which results in a monoaster comprised of two half-spindles and the arrest of cells in early mitosis with an active checkpoint (Mayer et al., 1999). A two-hour incubation of non-synchronized cells is preferred to induce a sufficient percentage of cells with monoasters while avoiding a prolonged mitotic arrest.

Table 1. Chemical inhibitors used in the protocol.

Agent		Stock solution*	Working concentration
Eg5 inhibitor	Monastrol	40 mM in DMSO	200 μM
	S-trityl-L-cysteine	20 mM in DMSO	20 μM
Cdk1 inhibitor	Roscovitine	50 mM in DMSO	50 μM
	Purvalanol A	25 mM in DMSO	25 μM

*Store all stock solutions in aliquots at -20 °C. The compounds are stable for at least 6 months.

1.2.3 Induction of cell division

Upon induction of asymmetrical monoasters, the subsequent step is to silence the spindle checkpoint and to initiate cytokinesis. Two different approaches have been shown to be effective. One was first described by Salmon and colleagues who microinjected a recombinant Mad1 deletion mutant into cells with monopolar spindles. Injected Mad1

protein then sequestered the spindle checkpoint protein Mad2 from kinetochores, thus bypassing the checkpoint and inducing precocious anaphase onset (Canman et al., 2003; Canman et al., 2002). Although labor-intensive and skill-demanding, microinjection is undoubtedly an excellent approach to deliver material into cells with precise timing and controlled dosage. Acute biological effects can be induced immediately by injection, which is particularly useful for studying a rapid and dynamic cellular process such as mitosis (usually complete within 2 h). In this case, the carry-over effects from interphase can be further avoided by injecting only the mitotic cells. Therefore, I have also taken advantage of this injection approach to induce asymmetrical cell division. I make microinjection needles from capillary glass pipettes using a micropipette puller. However, ready-to-use microinjection needles are also available from several vendors (e.g., Femtotips from Eppendorf). The precise settings for the microinjector depend on the needle, the injected sample and the cell line. I suggest an injection pressure of 90-150 hPa and an injection time of 0.2-0.3 s.

Alternatively, asymmetrical cell division is also triggered by the direct inhibition of the master mitotic kinase Cdk1 (Hu et al., 2008; Niiya et al., 2005). Addition of a Cdk1 inhibitor such as roscovitine or purvalanol A (Table 1) induces the formation and ingression of the cleavage furrow within 30 min of the treatment. Compared to the microinjection approach, induction of asymmetrical division by the addition of a chemical inhibitor is much easier and less time-consuming. The timing of drug addition and its potential off-target effects, however, need to be taken into consideration.

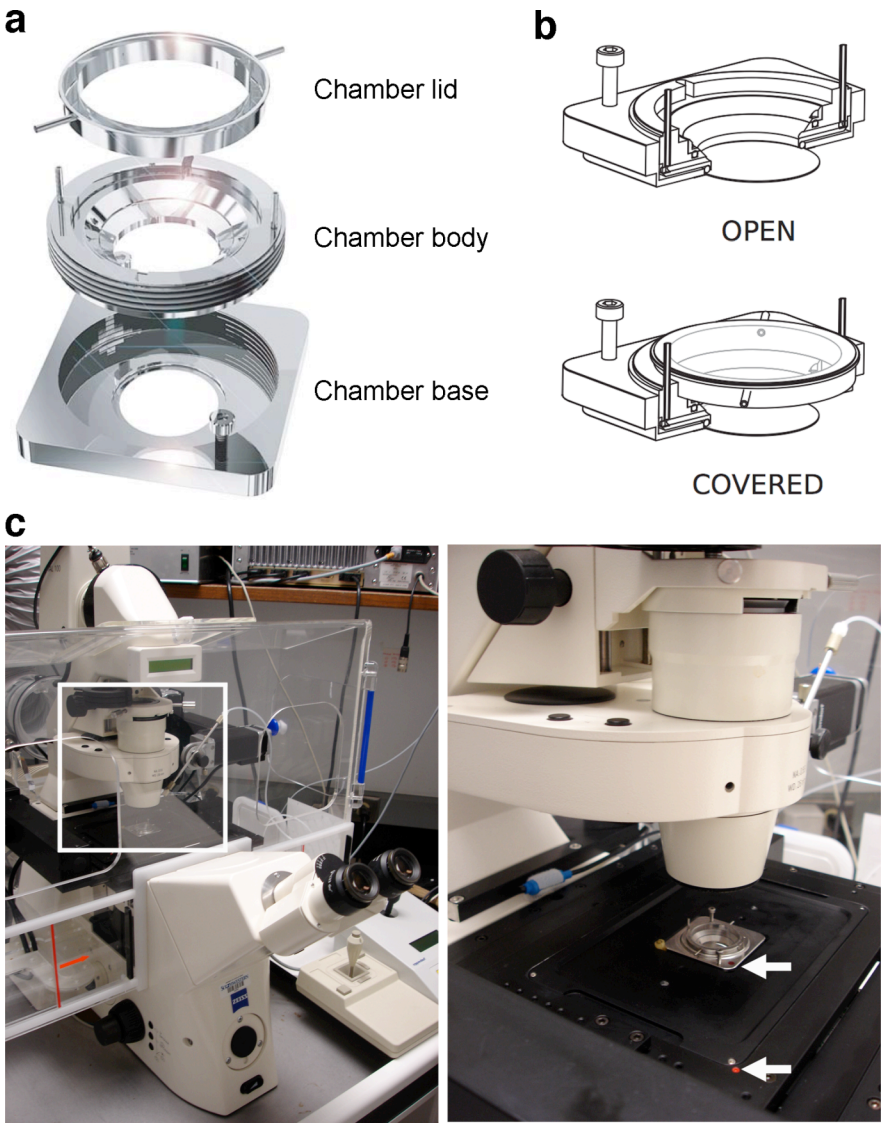

Figure 2. Setup of the Ludin imaging chamber. (a) Three main parts of the Ludin imaging chamber. The coverslip should be mounted into the chamber base with an O-ring placed onto the coverslip. The chamber body is then screwed onto the base and covered by the lid. (b) The two chamber configurations used in the protocol. The open configuration is used for microinjection, while the chamber is covered during live cell imaging to avoid evaporation of the medium. (c) Setup of the assembled Ludin chamber on the microscope. The orientation of the chamber on the stage is facilitated by the alignment of the red mark on the chamber with the one on the stage frame (pointed by arrows). Panels a and b are reproduced with permission of Dr. Beat Ludin.

1.2.4 Phase-contrast video microscopy

To identify cells with monoasters that divide asymmetrically into a karyoplast and a cytoplast, I follow the division process by phase-contrast video microscopy and relocate the karyoplast and cytoplast based on the XY stage positions recorded during live cell imaging. In the case of the injection-based approach, dividing cells can be monitored by video microscopy as well. However, if the access to live cell imaging equipment is limited, co-injection of a marker (e.g., fluorophore or biotin-conjugated dextran) together with Mad1 protein can be used instead to identify the karyoplast and the cytoplast (Wang et al., 2003; Wang et al., 2008b). In this case, recording of the stage positions and live cell imaging are not necessary since the divided cells can be identified by the injection marker (Wang et al., 2003; Wang et al., 2008b). Once asymmetrical cell division is complete, I either perform additional assays on the divided karyoplast and/or cytoplast, or directly process the cells for immunofluorescence or electron microscopy.

Precise retrieval of the original positions of the target cells among a large cell population is a major concern when performing correlative microscopy. Using a Ludin imaging chamber mounted onto a motorized scanning stage (Figure 2), the stage positions of dividing or divided cells can be precisely located during (Figure 3e-h) and after live cell imaging (Figures 4 and 5). The main advantage of the Ludin chamber is its design that allows us to efficiently correlate phase-contrast with immunofluorescence images. I first capture phase-contrast images of the dividing cells by video microscopy and record the corresponding XY coordinates of the stage positions using the microscope software. Upon completion of the assay, I remove the chamber from the stage and perform

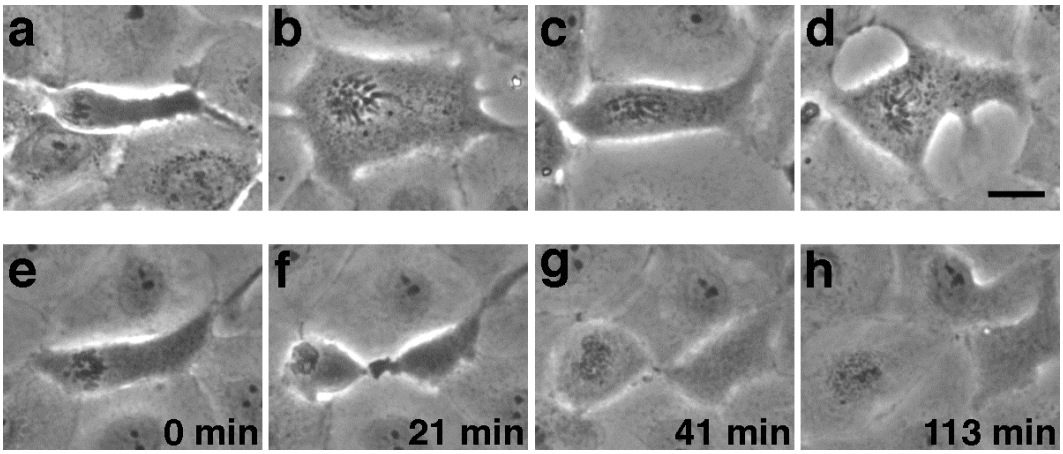

Figure 3. Monitoring of asymmetrical cell division. PtK1 cells were first treated for 2 h with 20 μM S-trityl-L-cysteine to generate asymmetrical monoasters. Asymmetrical cell division was then induced by addition of 25 μM purvalanol A. (a-d) Examples of cells with asymmetrical monoasters. (a) A cell with a typical asymmetrical monoaster that likely undergoes monopolar cytokinesis and generates a large cytoplast. Cells with a lower length-to-width ratio (b), a more centralized monoaster (c), or less contact with surrounding cells (d) may also divide but generate smaller-sized cytoplasts. (e-h) Consecutive still images taken from a phase-contrast video showing an asymmetrical cell division process. The cleavage furrow robustly assembles within 30 min upon induction of cell division (f). Scale bar, 20 µm.

immunostaining directly in the assembled chamber, which is then placed back onto the stage frame in the original orientation (Figure 2c). Since the chamber is square and accurately machined to fit into the holder, the cells are relocated virtually to the same positions as before the staining procedure. Thus, by revisiting the initial XY coordinates recorded by the software, multiple positions can be quickly and efficiently revisited to acquire correlative immunofluorescence images (for typical results, see Figure 4). Similar results can also be obtained using coverslips with an etched grid (e.g., Cellocate coverslips from Eppendorf). The disadvantage is that these coverslips are expensive and limited to a single use only. Moreover, since the coverslips are round, it is not possible to

remount them onto the stage to the same position as before the IF staining. Individual coordinates need to be searched and revisited manually, which is more time-consuming.

1.2.5 Immunofluorescence

To determine the requirement of the spindle in Golgi partitioning, I immunolabel the Golgi and microtubules and stain the DNA to visualize the nucleus (Figure 4). In the

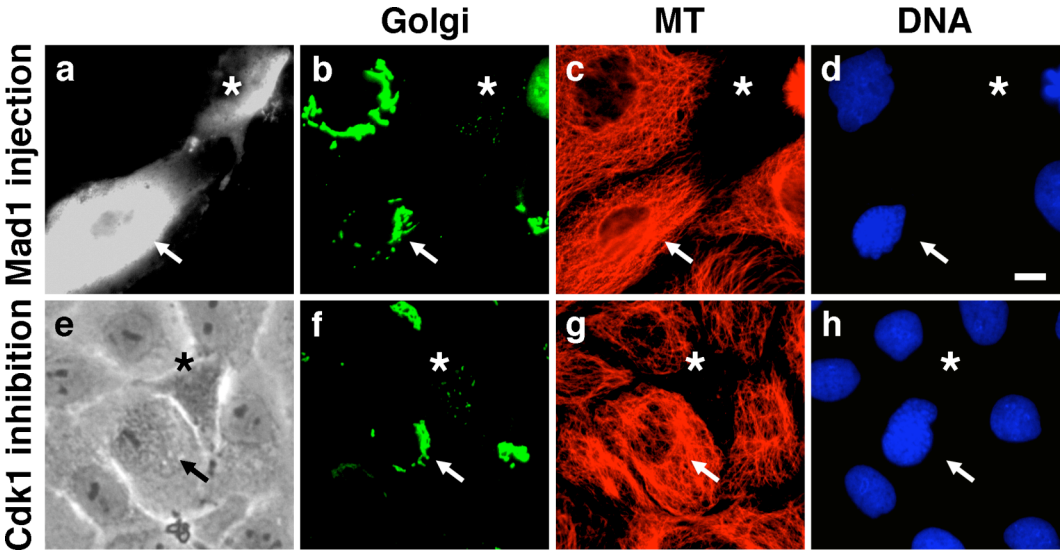

Figure 4. Correlative immunofluorescence images. PtK_1 cells were first treated for 2 h with 20 μM S-trityl-L-cysteine to generate asymmetrical monoasters. Asymmetrical cell division was then induced by microinjection of 1.5 mg ml^{-1} Mad1 (a-d) or by addition of 25 μM purvalanol A (e-h). The divided cells were identified by labeling the injection marker biotin-dextran, with Alexa Fluor 350-conjugated streptavidin (a) or by tracking the cells using phase-contrast time-lapse microscopy (e). Upon asymmetrical cell division, the cells were processed for immunofluorescence. The Golgi marker NAGT1-GFP (Golgi, green) was stained with antibodies against GFP followed by Alexa Fluor 488-conjugated secondary antibodies in b and f. Microtubules (MT, red) were labeled with an antibody against α-tubulin followed by Alexa Fluor 555-conjuagted secondary antibodies in c and Alexa Fluor 594-conjuagted secondary antibodies in g. The nuclei (DNA, blue) were stained with DRAQ5 in d and Hoechst in h. The karyoplasts are marked by arrows and arrowheads indicate the cytoplasts. Scale bar, 10 µm.

microinjection approach, the injection marker biotin-dextran is further labeled with Alexa Fluor-conjugated streptavidin to detect the injected cells. Upon completion of the assay, the cells are either directly fixed and permeabilized with methanol or first fixed with formaldehyde and then permeabilized with methanol. The choice of the fixation method depends on the antigen to be detected and the antibody that is used. I suggest using methanol for microtubule labeling as it gives a much cleaner network pattern. After fixation, I then perform immunostaining directly in the imaging chamber at 37 °C with antibodies against the Golgi marker NAGT1-GFP and α-tubulin. Although the immunostaining can be performed at room temperature (20-25 °C), incubation at 37 °C in a humidified tissue culture incubator (Lazarides and Weber, 1974) has three advantages. First, the antibody solution will not evaporate in the humidified atmosphere. Second, the dark environment protects the fluorophore from bleaching. Third, unspecific binding of antibodies is reduced at 37 °C, resulting in a better signal-to-noise ratio. This may significantly improve the staining if the affinity of the antibodies is low. The nucleus is stained either with the DNA dye Hoechst or with a far red-emitting DNA probe DRAQ5. I suggest a brief treatment with RNase A prior to DRAQ5 staining to minimize the background signal from RNA.

1.2.6 Electron microscopy

To obtain correlative electron micrographs (for typical results, see Figure 5), the majority of cells except those surrounding the target cells are scraped off the coverslip with a microinjection needle using a micromanipulator (Jokitalo et al., 2001; Wang et al., 2003; Wang et al., 2008b), leaving behind few layers of cells that appear as individual “cell

islands" (Figure 5a). I normally make up to 3 cell islands that are located in close proximity and near the center of the coverslip. These cell islands can be clearly seen while trimming the resin block and readily recognized under the electron microscope at low magnification (Figure 5d). Once the target cells are identified, correlative EM images can be acquired at higher magnification (Figure 5e-g).

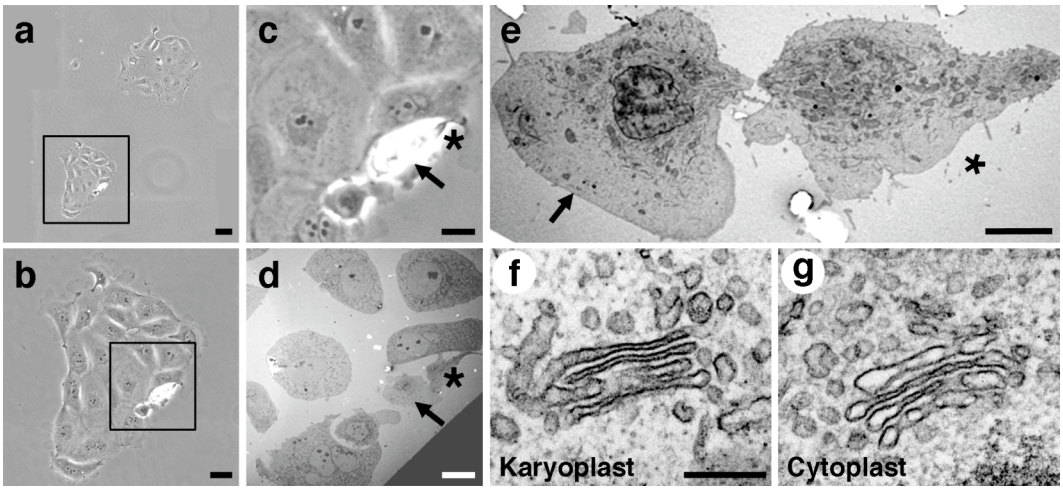

Figure 5. Correlative electron micrographs. Phase-contrast images of the divided cells used to identify the target cells under the electron microscope (a-c). (a) Image of individual cell islands assembled from adjacent fields. Scale bar, 80 μm. (b,c) Magnified images of the cell island in a. Scale bars, 40 μm in b and 20 μm in c. (d) A low-magnification correlative electron micrograph of the phase-contrast image c. The arrow marks the karyoplast and the asterisk indicates the cytoplast. Scale bar, 20 μm. (e) A different thin section of the same cell pair as in d, showing a karyoplast and a cytoplast in the early post-division stage. Scale bar, 5 μm. (f,g) The karyoplast and the cytoplast show stacked Golgi cisternae at high magnification. Scale bar, 0.2 μm.

2. Materials

2.1 Reagents

Alcian blue 8GX (Sigma, cat. no. A5268)

Biotin-dextran, lysine fixable, MW 70,000 (Invitrogen, cat. no. D-1957)

Bovine serum albumin (BSA), Fraction V (Fisher Scientific, cat. no. BP1605-100)

CO_2-independent medium (Invitrogen, cat. no. 18045-088)

DRAQ5 (Biostatus, cat. no. DR50200)

!CAUTION Toxic if ingested, inhaled, or absorbed through the skin. Wear gloves and avoid any contact with the skin.

EMbed 812 kit including EMbed 812, DDSA, NMA and DMP-30 (Electron Microscopy Sciences, cat. no. 14120)

!CAUTION DDSA and DMP-30 are harmful. NMA is toxic and extremely irritating. Use in a chemical hood.

Ethanol

Formaldehyde solution, 36.5-38% (wt/vol) (Mallinckrodt, cat. no. 5016-02)

!CAUTION Harmful. Use in a chemical hood.

Glutaraldehyde solution, 25% (wt/vol) (Electron Microscopy Sciences, cat. no. 16220)

!CAUTION Toxic. Use in a chemical hood.

Ham's F-12 medium (Mediatech, Inc., cat. no. 50-040-PB)

HEPES (Fisher Scientific, cat. no. BP310-500)

Hoechst 33342 (Invitrogen, cat. no. H-21492)

!CAUTION Potentially mutagenic. Wear gloves and avoid any contact with the skin.

Hydrofluoric acid solution, 48% (wt/vol) (Mallinckrodt, cat. no. 2640)

!CAUTION Corrosive and extremely hazardous. Wear appropriate personal protective equipment and handle in a chemical hood with extreme caution. Neutralize waste acid with sodium carbonate.

Lead nitrate (Electron Microscopy Sciences, cat. no. 17900)

!CAUTION Highly toxic if ingested, inhaled, or absorbed through the skin. Wear gloves and handle in a chemical hood.

Methanol (Fisher Scientific, cat. no. BP1105-4)

!CAUTION Methanol may be fatal or cause blindness if swallowed. Harmful if inhaled or absorbed through the skin. Wear gloves and handle in a chemical hood.

Monastrol (Biomol, cat. no. GR-322)

Mowiol 4-88 (Calbiochem, cat. no. 475904)

Osmium tetroxide solution, 2% (wt/vol) (Electron Microscopy Sciences, cat. no. 19152)

!CAUTION Highly toxic, even at low levels of exposure. Handle in a chemical hood with appropriate precautions.

Potassium ferricyanide (Sigma, cat. no. P8131)

!CAUTION Slightly hazardous if ingested, inhaled, or absorbed through the skin. Wear gloves and handle in a chemical hood.

Primary mouse monoclonal antibody against α-tubulin (TAT1) (Seemann et al., 2002)

Primary rabbit polyclonal antibodies against GFP (Pelletier et al., 2002)

Propylene oxide (Electron Microscopy Sciences, cat. no. 20401)

!CAUTION Extremely flammable. Use in a chemical hood and avoid any open flame.

Purvalanol A (Calbiochem, cat. no. 540500)

Rat kangaroo (Potorous tridactylis) kidney epithelial cells, PtK_1 (ATCC, no. CRL-6493)

Recombinant Mad1 protein (GST-tagged Mad1 a.a. 321-556)

RNase A, DNase-free (Qiagen, cat. no. 19101)

Roscovitine (Calbiochem, cat. no. 557360)

Secondary Alexa Fluor 488 goat anti-rabbit antibodies (Invitrogen, cat. no. A-11034)

Secondary Alexa Fluor 555 goat anti-mouse antibodies (Invitrogen, cat. no. A-21424)

Secondary Alexa Fluor 594 goat anti-mouse antibodies (Invitrogen, cat. no. A-11032)

Sodium cacodylate (Electron Microscopy Sciences, cat. no. 12300)

!CAUTION Highly toxic and may be fatal by ingestion, inhalation, or skin absorption. Wear gloves and avoid any contact with the skin.

Sodium carbonate (Mallinckrodt, cat. no. 7527-04)

Sodium citrate (Electron Microscopy Sciences, cat. no. 21140)

!CAUTION Slightly hazardous if ingested, inhaled, or absorbed through the skin. Wear gloves and handle in a chemical hood.

Streptavidin-Alexa Fluor 350 (Invitrogen, cat. no. S-11249)

S-trityl-L-cysteine (Acros Organics, cat. no. 173010050)

Uranyl acetate (Electron Microscopy Sciences, cat. no. 22400)

!CAUTION Harmful if ingested, inhaled, or absorbed through the skin. Wear gloves and handle in a chemical hood.

2.2 Equipment

Aluminum dishes (Electron Microscopy Sciences, cat. no. 70048-01)

Axiovert 200M motorized inverted microscope (Zeiss)

Diamond knife (Diatome)

Embedding (BEEM) capsules (Electron Microscopy Sciences, cat. no. 70000-B)

Glass capillaries (Sutter Instrument, cat. no. BF100-78-10)

Glass coverslips, round, 15 mm in diameter, #1 (Daigger, cat. no. EF15973B)

Glass coverslips, round, 18 mm in diameter, #1.5 (Fisher Scientific)

Loading tips for microinjection, 10 µl (Fisher Scientific, cat. no. 02-707-88)

Ludin imaging chamber (Life Imaging Services)

Ludin imaging chamber-mounting frame (Life Imaging Services)

Microinjector FemtoJet (Eppendorf)

Micromanipulator 5171 (Eppendorf)

Micropipette puller P-97 (Sutter Instrument)

Microscope incubation system including incubator XL-3, heating unit and tempcontrol 37-2 digital (Zeiss)

Motorized scanning stage (Märzhäuser Wetzlar)

Nickel grids, formvar-coated, 200 mesh (Electron Microscopy Sciences, cat. no. FF200-Ni)

Objective A-PLAN 20x/0.3 PH1 (Zeiss)

Objective LD Plan-Neofluar 40x/1.3 DIC (Zeiss)

Openlab 4.0.2 imaging software (Improvision)

Orca-285 CCD camera (Hamamatsu)

Razor blades

Tecnai G2 Spirit transmission electron microscope (FEI Company)

Ultramicrotome (Ultracut E, Leica)

USC1000 2k CCD camera (Gatan)

2.3 Reagent setup

Alcian blue solution 0.1% (wt/vol) Alcian blue in H_2O. Store at 4 °C in the dark. The solution is stable for 6 months. Discard if precipitates form.

Biotin-dextran stock solution 50 mg ml^{-1} in H_2O. The stock can be stored at 4 °C for at least 6 months. Use 2.5 mg ml^{-1} for microinjection.

Blocking buffer for IF 1 mg ml^{-1} BSA in PBS. The buffer can be stored at 4 °C for several weeks.

Cdk1 inhibitor stock solution 50 mM roscovitine or 25 mM purvalanol A dissolved in DMSO. Store in aliquots at -20 °C. The compounds are stable for at least 6 months.

Cell culture medium F-12 medium containing 10% (vol/vol) cosmic calf serum (CCS, Hyclone) or fetal calf serum (FBS), 100 units ml^{-1} penicillin, 100 µg ml^{-1} streptomycin and 2 mM glutamine.

DRAQ5 stock solution 5 mM in diluted acid. Store at 4 °C in the dark. The solution is stable for at least 6 months. Use at 1-2.5 µM.

!CAUTION Toxic if ingested, inhaled, or absorbed through the skin. Wear gloves and avoid any contact with the skin.

Eg5 inhibitor stock solution 40 mM monastrol or 20 mM S-trityl-L-cysteine dissolved in DMSO. Store in aliquots at -20 °C. The compounds are stable for at least 6 months.

Embedding solution Mix 22.0 g of EMbed 812, 14.8 g of NMA and 9.0 g of DDSA until no streaks are left. Add 0.7 g of DMP-30 and mix again. Prepare fresh on the day of use.

!CAUTION DDSA and DMP-30 are harmful. NMA is toxic and extremely irritating. Use in a chemical hood.

Ethanol 50%, 70%, 90%, 95% and 100% (vol/vol) ethanol in H_2O. Prepare fresh on the day of use.

Fixative for EM 2.5% (wt/vol) glutaraldehyde in 100 mM sodium cacodylate, pH 7.4. Dilute fresh on the day of use.

!CAUTION Glutaraldehyde is toxic. Use in a chemical hood. Sodium cacodylate is highly toxic and may be fatal by ingestion, inhalation, or skin absorption. Wear gloves and avoid any contact with the skin.

Fixative for IF 3.7% (wt/vol) formaldehyde in PBS. Dilute fresh on the day of use.

!CAUTION Harmful. Use in a chemical hood.

Hoechst stock solution 1 mg ml^{-1} Hoechst 33342 in H_2O. Store at 4 °C in the dark. The solution is stable for at least 6 months. Use at 1 µg ml^{-1}.

!CAUTION Potentially mutagenic. Wear gloves and avoid any contact with the skin.

Hydrofluoric acid solution The solution should be stored in a chemical hood at room temperature and separated from other chemicals. Carefully transfer 1.5 ml into a 15 ml conical tube and pre-chill at 4 °C on the day of use.

!CAUTION Corrosive and extremely hazardous. Wear appropriate personal protective equipment and handle in a chemical hood with extreme caution. Neutralize waste acid with sodium carbonate.

Imaging medium for live cell imaging and microinjection Cell culture medium containing 50 mM HEPES, pH 7.4 or CO_2-independent medium supplemented with 10%

(vol/vol) CCS or FBS, 100 units ml^{-1} penicillin, 100 µg ml^{-1} streptomycin and 2 mM glutamine.

Lead citrate solution (Reynolds, 1963) Dissolve 1.33 g of lead nitrate and 1.76 g of sodium citrate in 30 ml of H_2O by vigorously shaking for 1 min. Let stand for 30 min with occasional mixing to ensure complete conversion to lead citrate. Add 8 ml of 1 N sodium hydroxide and dilute to 50 ml with H_2O. The final pH should be around 12. The solution can be stored at room temperature for 6 months.

!CAUTION Lead nitrate is highly toxic and sodium citrate is slightly hazardous if ingested, inhaled, or absorbed through the skin. Wear gloves and handle in a chemical hood.

Methanol Pre-chill and store at -20 °C.

!CAUTION Methanol may be fatal or cause blindness if swallowed. Harmful if inhaled or absorbed through the skin. Wear gloves and handle in a chemical hood.

Mowiol mounting solution Mix 6 g of glycerol, 2.4 g of Mowiol 4-88 and 6 ml of H_2O. Stir for 2 h at room temperature. Add 12 ml of 0.2 M Tris-HCl, pH 8.5 and incubate at 53 °C with occasional mixing until dissolved. The solution can be stored at room temperature for several days or in aliquots at -20 °C for at least 6 months.

Osmium tetroxide buffer 1% (wt/vol) osmium tetroxide and 1.5% (wt/vol) potassium ferricyanide in 100 mM sodium cacodylate, pH 7.4. Prepare fresh on the day of use.

!CAUTION Osmium tetroxide is highly toxic, even at low exposure levels. Handle in a chemical hood with appropriate precautions. Potassium ferricyanide is slightly hazardous if ingested, inhaled, or absorbed through the skin. Wear gloves and handle in a chemical

hood. Sodium cacodylate is highly toxic and may be fatal by ingestion, inhalation, or skin absorption. Wear gloves and avoid any contact with the skin.

Recombinant Mad1 protein The oligomerization and Mad2- binding domain of Mad1 (residues 321-556) (Canman et al., 2002) was cloned from IMAGE clone 4299982 (ATCC) into pGEX4-T3, purified on glutathione-Sepharose 4B (GE Healthcare), dialyzed against injection buffer (20 mM HEPES, pH 7.4 and 50 mM KOAc) and concentrated on a Centricon YM-30 filtration unit (Wei and Seemann, 2009). Store in aliquots at -80 °C. Aliquots are stable for at least 6 months. Use 1.5 mg ml^{-1} for microinjection.

2.4 Equipment setup

Alcian blue-coated coverslips (Hammond and Helenius, 1994) Wash coverslips four times, alternating with 20-30 ml of water and ethanol. Add Alcian blue solution and boil for 30 s in a microwave oven. Leave the coverslips to cool and then wash with 20-30 ml of water and air-dry in a tissue culture hood or sterilize by flaming.

Electron microscopy setup Electron micrographs are acquired on a Tecnai G2 Spirit transmission electron microscope at 120 kV with a USC1000 2k CCD camera.

Live cell imaging and fluorescence microscopy setup Phase-contrast images are acquired at intervals of 3-12 min with an A-PLAN 20x/0.3 PH1 objective on an Axiovert 200M microscope equipped with an Orca-285 camera and the imaging software Openlab 4.0.2. Correlative immunofluorescence images are acquired using an LD Plan-Neofluar 40x/1.3 DIC objective on the same microscope.

Microinjection setup Perform microinjection with a Microinjector FemtoJet and a Micromanipulator 5171 connected to an Axiovert 200M microscope (Bartz et al., 2008).

3. Procedure

3.1 Preparation of cells and the imaging system ● TIMING 2 d

1 | Grow PtK_1 cells in F-12 cell culture medium in an incubator at 37 °C, 5% CO_2. Plate approximately 3 x 10^5 cells into a 35 mm dish containing 2 ml of cell culture medium and an Alcian blue-coated 18 mm round glass coverslip. Grow the cells to full confluency.

▲ CRITICAL STEP Full cell confluency and coating of the glass coverslips enhance the occurrence of asymmetrical cell division.

2 | Turn on the heating unit and the temperature controller of the microscope incubation system. Maintain the temperature at 37 °C for at least 3 h before the experiment. I recommend switching on the heating unit the night before the experiment. Let the system stand by until Step 4.

▲ CRITICAL STEP The temperature at the stage center of the microscope should be in equilibrium with the surroundings and stabilized at 37 °C. Temperature fluctuations may cause focus drifts.

3.2 Generation of asymmetrical monoasters ● TIMING 2 h

3 | Remove the cell culture medium. Briefly wash the cells twice with 2 ml of imaging medium. Treat the cells for 2 h at 37 °C with an Eg5 inhibitor (200 µM monastrol or 20 µM S-trityl-L-cysteine in 1 ml of imaging medium).

3.3 Induction of asymmetrical cell division ● TIMING 30 min

4| Mount the coverslip into the Ludin imaging chamber. Place an O-ring onto the coverslip and screw the chamber body onto the chamber base (Figure 2a). Gently rinse the cells twice with 1 ml of imaging medium containing the Eg5 inhibitor. Remove the imaging medium and add another 1 ml of fresh imaging medium containing the Eg5 inhibitor. Place the lid onto the chamber and make sure that it is properly sealed. Upon full assembly of the imaging chamber, wipe the bottom of the coverslip with ethanol to remove residual medium. Place the Ludin imaging chamber onto the microscope stage and let it sit for few min to equilibrate the temperature.

▲ CRITICAL STEP Assemble the imagine chamber as fast as possible and never let the cells dry out.

5| Trigger asymmetrical cell division by microinjection of recombinant Mad1 protein (option A) or by addition of a Cdk1 inhibitor (option B).

▲ CRITICAL STEP I observe that the cells start to form a cleavage furrow within 30 min of treatment. Therefore, the time to identify the target cells should not exceed 30 min if the entire division process should be recorded.

(A) Microinjection of recombinant Mad1 protein ● TIMING 30 min

(i) Pull microinjection needles from capillary glass using a micropipette puller according to the manufacturer's instructions. Micropipettes can be stored resting on a small roll of plasticine or a double-sided tape in a flat, covered container.

(ii) Thaw an aliquot of recombinant Mad1 protein on ice. Centrifuge the protein using a microcentrifuge for 15 min at 10,000*g*, 4 °C prior to loading the supernatant into the microinjection needle.

▲ CRITICAL STEP Centrifugation before loading into the needle clears the injection solution and prevents clogging of the needle.

(iii) Carefully remove the lid from the imaging chamber to access the cells for subsequent microinjection. Bring cells into the focus using phase-contrast illumination.

(iv) Load 1-2 µl of Mad1 protein into the back end of the microinjection needle using a loading tip. Attach the microinjection needle to the needle holder and mount onto the microinjector. Using the micromanipulator, lower the needle and immerse the tip into the imaging medium.

▲ CRITICAL STEP Avoid prolonged exposure of the loaded needle to the air, which may cause evaporation of the injection solution and thus clogging of the tip.

(v) Move the tip using the micromanipulator into the field of view at low magnification. Change to higher magnification. Slowly and carefully lower the tip to just above the cells. Be careful not to touch the glass surface as this may cause the tip to break.

(vi) Inject recombinant Mad1 protein into cells with an asymmetrical monoaster.

? TROUBLESHOOTING

(vii) Record the stage positions for each injected cell.

(viii) After finishing all injections, place the lid back onto the imaging chamber and start live cell imaging.

(B) Addition of a Cdk1 inhibitor ● TIMING 30 min

(i) Carefully open the lid and remove the medium with a syringe or pipette.

(ii) Add 1 ml of fresh imaging medium containing the Eg5 inhibitor and a Cdk1 inhibitor (25 µM purvalanol A or 50 µM roscovitine). Place the lid back onto the chamber. Alternatively, the medium can be exchanged with a peristaltic pump or a syringe through the perfusion lines of the Ludin imaging chamber.

(iii) Identify the cells with asymmetrical monoasters using phase-contrast illumination (for typical morphology of asymmetrical monoasters, see Figure 3). Record the XY coordinates of the stage. Start time-lapse imaging and revisit each recorded position at each time point.

3.4 Phase-contrast time-lapse microscopy ● TIMING 2 h

6| Continue time-lapse imaging for 2 h and monitor the asymmetrical division process.

? TROUBLESHOOTING

3.5 Processing for correlative immunofluorescence or electron microscopy

7| Upon completion of asymmetrical cell division, the divided cells are prepared for correlative immunofluorescence (option A) or correlative electron microscopy (option B). Alternatively, the cells can be subjected to other assays prior to processing.

(A) Correlative immunofluorescence microscopy ● TIMING 2 h

(i) Remove the Ludin chamber from the microscope stage. Take the lid off but do not disassemble the imaging chamber. The entire staining procedure should be performed directly in the Ludin chamber. Aspirate the imaging medium and fix and permeabilize the cells with 2 ml of pre-chilled -20 °C methanol for 10 min at -20 °C. Alternatively, the cells can be fixed with 2 ml of 3.7% (wt/vol) formaldehyde in PBS for 15 min at room temperature and then permeabilized with 2 ml of pre-chilled -20 °C methanol for 10 min at -20 °C.

!CAUTION Methanol may be fatal or cause blindness if swallowed. Harmful if inhaled or absorbed through the skin. Wear gloves and handle in a chemical hood. Formaldehyde is a harmful chemical. Prepare fixative in a chemical hood.

■ PAUSE POINT The sample can be left in methanol at -20 °C from 10 min to overnight.

(ii) Aspirate the methanol and rehydrate the cells in 2 ml of PBS for 5 min at room temperature.

(iii) Briefly rinse with 2 ml of PBS. Remove the PBS and place the Ludin chamber into a humidified chamber to prevent evaporative losses. Block with 150 µl of blocking buffer for 15 min at 37 °C.

▲ CRITICAL STEP All 37 °C incubations of the immunostaining steps should be done in a humidified tissue culture incubator to minimize evaporation and light exposure.

(iv) Wash three times with 2 ml of PBS.

(v) Stain with 150 µl of primary antibodies (rabbit anti-GFP and mouse anti-α-tubulin) in blocking buffer for 30 min at 37 °C. I suggest using 0.5-2 µg ml^{-1} of purified antibody or 1:200-1:600 dilutions for serum.

(vi) Wash three times with 2 ml of PBS.

(vii) Stain with 150 µl of secondary antibodies in blocking buffer for 30 min at 37 °C. I suggest using 1:300 dilutions for the Alexa Fluor-conjugated secondary antibodies.

(viii) Wash three times with 2 ml of PBS.

(ix) Stain the nuclei with 150 µl of Hoechst or DRAQ5 in blocking buffer for 5 min at 37 °C. Prior to DRAQ5 staining, treat samples with 150 µl of 0.1 mg ml^{-1} RNase A in PBS for 5 min at 37 °C.

!CAUTION Hoechst is potentially mutagenic. DRAQ5 is toxic if ingested, inhaled, or absorbed through the skin. Wear gloves and avoid any contact with the skin.

(x) Wash three times with 2 ml of PBS.

(xi) Add 150 µl of Mowiol mounting solution. Place a 15 mm round coverslip on top of the Mowiol solution and avoid air bubbles during mounting. Gently tap on the coverslip using tweezers and aspirate the excess mounting solution from the edge. Incubate for at least 5 min at room temperature in the dark to allow the mounting solution to harden.

■ PAUSE POINT The sample should be stored in the dark from this step on. Although the sample is stable for several weeks, it is advised to examine the sample at the earliest time.

(xii) Place the imaging chamber back onto the microscope stage. Reposition the stage to the XY coordinates recorded during the live cell imaging. Acquire fluorescence images for each recorded position using the appropriate fluorescence filter sets.

(B) Correlative electron microscopy ● TIMING 2 d

(i) Remove the lid but do not disassemble the imaging chamber. Locate the target cells by repositioning the stage to the recorded XY coordinates. As an alternative to video microscopy, target cells can be located using a microgrid coverslip (van Rijnsoever et al., 2008), or a regular coverslip with a roughly 2 mm x 2 mm square marked with a diamond knife (Uchiyama et al., 2006).

(ii) Scrape off the majority of the cells except those surrounding the target cells with a microinjection needle using the micromanipulator (Jokitalo et al., 2001; Wang et al., 2008b). Leave one or two layers of neighboring cells behind to ensure the integrity of the target cells.

(iii) Transfer the coverslip from the Ludin chamber into a 35 mm dish. Fix the cells with 3 ml of 2.5% (wt/vol) glutaraldehyde in 100 mM sodium cacodylate, pH 7.4 for 30 min at room temperature.

!CAUTION Glutaraldehyde is a toxic chemical. Prepare fixative in a chemical hood. Sodium cacodylate contains arsenic and may be carcinogenic. It is highly toxic and may be fatal by ingestion, inhalation, or skin absorption. Wear gloves and avoid any contact with the skin.

(iv) Replace with 3 ml of fresh fixative, seal the dish with parafilm and store at 4 °C overnight.

(v) Wash three times with 2 ml of 100 mM sodium cacodylate, pH 7.4.

(vi) Postfix the sample with 2 ml of osmium tetroxide buffer for 30-50 min at room temperature.

!CAUTION Osmium tetroxide is highly toxic, even at low exposure levels. Handle in a chemical hood with appropriate precautions.

(vii) Wash three times with 2 ml of 100 mM sodium cacodylate, pH 7.4.

(viii) Dehydrate the cells in a graded ethanol series. Immerse the sample in 2 ml of 50% (vol/vol) ethanol three times for 2-5 min each, 2 ml of 70% (vol/vol) ethanol three times for 2-5 min each, 2 ml of 90% (vol/vol) ethanol once for 2-5 min, and then 2 ml of 95% (vol/vol) ethanol twice for 5-10 min each. Transfer the coverslip to an aluminum dish. Immerse the sample in 5-10 ml of 100% (vol/vol) ethanol three times for 5-10 min each.

▲ CRITICAL STEP Do not let the cells dry out during the embedding process.

(ix) Place the sample in 5-10 ml of propylene oxide for 10 min. Cover the aluminum dish with a glass lid.

!CAUTION Propylene oxide evaporates very quickly and is extremely flammable. Use in a chemical hood and avoid any open flame. Since propylene oxide dissolves plastic dishes, the coverslip should be transferred into an aluminum dish and covered with a glass lid.

(x) Freshly prepare embedding solution as described in the REAGENT SETUP. Freshly prepare a 1:1 mixture of embedding solution and propylene oxide.

!CAUTION Prepare and store all solutions in a chemical hood. Subsequent embedding steps should be performed in a chemical hood as well.

(xi) Incubate the cells with 5-10 ml of 1:1 mixture of embedding solution and propylene oxide for 1 h at room temperature. Remove the majority of the solution but leave a thin layer to cover the coverslip. Then incubate with 5-10 ml of embedding solution for at least 2 h at room temperature. Cover with a lid during the entire incubation process.

(xii) Remove the excess embedding solution from the aluminum dish and leave the coverslip covered by a thin layer of embedding solution. Fill an embedding capsule with embedding solution and place it upside-down onto the coverslip. Position the capsule so that region of interest is located at the center of the resin block.

(xiii) Place in an oven at 60 °C overnight to polymerize the resin.

■ PAUSE POINT The sample can be stored at room temperature until sectioning.

(xiv) Remove the resin block from the aluminum dish and remove the embedding capsule. Gently scrape the thin layer of resin off the coverslip with a razor blade until the glossy glass surface is revealed. Remove the glass coverslip by dipping the resin block into liquid nitrogen. If some glass fragments remain, immerse the resin block with the glass surface facing down into 1.5 ml of pre-chilled hydrofluoric acid in a 15 ml conical tube (Moore, 1975). Wait until the glass is completely dissolved (5-15 min) and then neutralize the residual hydrofluoric acid by carefully immersing the block into a large volume of saturated sodium carbonate solution.

!CAUTION Hydrofluoric acid is corrosive and extremely hazardous. Wear appropriate personal protective equipment including lab coat, safety goggles and gloves. Handle hydrofluoric acid in a chemical hood with extreme caution. Be aware that hydrofluoric acid will react violently with sodium carbonate and produce a copious amount of carbon dioxide gas (bubbles).

(xv) Trim the block to the area of the cell islands and cut thin sections parallel to the cell monolayer using a diamond knife and an ultramicrotome. Collect thin sections onto Formvar-coated grids. Contrast sections with 2% (wt/vol) uranyl acetate for 10 min and

lead citrate solution for 5 min. Wash grids with water and let dry. This step may require the help of an experienced electron microscopist.

!CAUTION Uranyl acetate and lead citrate solution are harmful if ingested, inhaled, or absorbed through the skin. Wear gloves and handle in a chemical hood.

■ PAUSE POINT The sections can be stored at room temperature until ready to acquire images.

(xvi) View sections under the electron microscope. Starting at low magnification, identify the target cells using pre-captured phase-contrast images as a road map. Upon identification of the target cells, acquire images at higher magnification.

3.6 Timing

Provided that cell cultures are ready for the assay and all necessary solutions are made, the entire procedure takes approximately 2 to 4 working days.

Step 1: Preparation of cell cultures: 1-2 d

Step 2: Warming up the microscope incubation system: ≥ 3 h

Step 3: Generation of asymmetrical monoasters: 2 h

Steps 4-5: Induction of asymmetrical cell division: 30 min

Step 6: Monitoring the cell division process: 2 h

Step 7: Processing for immunofluorescence (A, 2 h) or electron microscopy (B, 2-4 d)

3.7 Troubleshooting

Table 2. Troubleshooting table.

Step	Problem	Possible reason	Solution
5A (vi)	The microinjection needle is clogged	Precipitates in the injection sample	Filter and centrifuge the injection sample prior to loading into the needle
			Increase the injection pressure or gently tap the needle to dislodge the blockage
		Sticky protein solution	Use a bee stinger-shaped needle
6	The incidence of asymmetrical division is low	Weak attachment of cells to the glass surface	Coat the glass coverslips with Alcian blue
		Lack of cell-cell contacts with neighboring cells	Grow cells to full confluency
6	Cytoplasts generated are small	Less polarized monoasters	Choose cells with the features described in the anticipated results and Figure 3
6	Focus drifts during time-lapse microscopy	Temperature fluctuations	Allow the temperature to equilibrate overnight

4. Anticipated results

A cell with a typical asymmetrical monoaster that likely undergoes monopolar cytokinesis is shown in Figure 3a. It is advised to target cells with a higher length-to-width ratio (Figure 3a vs. 3b), a more polarized monoaster (Figure 3a vs. 3c), and broader contacts with surrounding cells (Figure 3a vs. 3d). The cells with the above characteristics more likely divide asymmetrically and generate larger cytoplasts that facilitate subsequent analysis. Figure 3e-h presents a series of consecutive still images taken from a phase-contrast video showing a typical asymmetrical division process.

Figures 4 and 5 illustrate typical results of asymmetrical cell division (Wei and Seemann, 2009). Figure 4 shows two sets of correlative immunofluorescence images of karyoplasts and cytoplasts, which were induced to divide by Mad1 microinjection (a-d) and by Cdk1 inhibition (e-h), respectively. The divided cells were identified either by labeling the injection marker biotin-dextran with Alexa Fluor 350-conjugated streptavidin (a) or by tracking the cells using phase-contrast time-lapse microscopy (e). Upon successful division, the cells were fixed and immunolabeled. The Golgi apparatus (Golgi, NAGT1-GFP), microtubules (MT, α-tubulin) and the nuclei (DNA) were stained and pseudo-colored in green, red and blue, respectively. In both cases, the nucleus and the microtubule network reformed in the karyoplasts but not in the cytoplasts. Moreover, the Golgi complex in the karyoplasts (indicated by arrows) reformed a ribbon-like structure in the perinuclear area, whereas the Golgi in the cytoplasts (marked by arrowheads) was dispersed in the cytoplasm. The failure in ribbon reassembly in the spindle-lacking

cytoplasts suggests that the spindle is required for the inheritance of a higher-order architecture of the Golgi apparatus.

Figure 5 shows a set of phase-contrast images and the correlative electron micrographs at different magnifications. The phase-contrast images (Figure 5a-c) were captured before fixation to allow unambiguous identification of the target cells under the electron microscope (Figure 5d). Figure 5e demonstrates a karyoplast and a cytoplast in the early post-division stage. At high magnification, stacked Golgi cisternae are clearly detectable in both the karyoplast and the cytoplast (Figure 5f,g), suggesting that stacked Golgi cisternae form independently of the spindle at the end of mitosis.

Chapter Three Results

The mitotic spindle mediates inheritance of the Golgi ribbon structure

1. Introduction

The Golgi apparatus in mammalian cells consists of stacks of flattened cisternae that are linked together laterally into a single continuous ribbon in the perinuclear region. As the central hub of the secretory pathway, the Golgi receives newly synthesized proteins from the ER and sorts them to their correct cellular destinations. The orientation of the Golgi ribbon directs exocytosis towards a particular area of the plasma membrane and thereby facilitates the establishment of cell polarity, for instance, during wound healing (Preisinger et al., 2004), neural development (Horton et al., 2005) and immune response (Stinchcombe et al., 2006).

During cell division, the single Golgi ribbon needs to be segregated into the two daughter cells. To achieve partitioning, the Golgi fragments at the onset of mitosis and later reforms in each daughter cell (Lowe and Barr, 2007). Two different mechanisms have been proposed for the partitioning of the Golgi. In one view, Golgi membranes are absorbed into and partitioned with the ER (Zaal et al., 1999). The second view argues that the Golgi remains distinct from the ER and the two compartments are inherited independently (Bartz and Seemann, 2008). In this scenario, the spindle has been proposed as the machinery responsible for Golgi partitioning, based on the observed accumulation

of Golgi membranes at the spindle poles (Shima et al., 1998) although a pool of membranes is dispersed throughout the cytoplasm (Jesch et al., 2001b).

To elucidate the role of the spindle in Golgi partitioning, I established an assay where the entire spindle is segregated into only one daughter cell. Upon division, a Golgi ribbon reformed in the karyoplasts, while the stacked cisternae were scattered throughout the cytoplasts. I could rescue ribbon assembly in the cytoplasts by microinjecting the Golgi extract together with tubulin or by lowering the division temperature, at which partial spindle materials were transferred into the cytoplasts. I propose that Golgi factors required for ribbon assembly rely on the spindle for partitioning, but functional stacks are inherited independently. This reveals two levels of regulation underlying Golgi inheritance. Coupling of these factors with the spindle would ensure that daughter cells receive the information to assemble the Golgi ribbon, which is vital for cellular functions that require polarized secretion and directional migration.

2. Results

To evaluate the role of the spindle in Golgi partitioning, I first examined the spatial correlation between Golgi membranes and the spindle. Consistent with previous reports (Jokitalo et al., 2001; Shima et al., 1998), I found Golgi membranes concentrated in metaphase around the two spindle poles in a variety of cell lines including HeLa, Vero, LLC-PK1, NRK and PtK1 (unpublished data). The association was prominent in PtK1

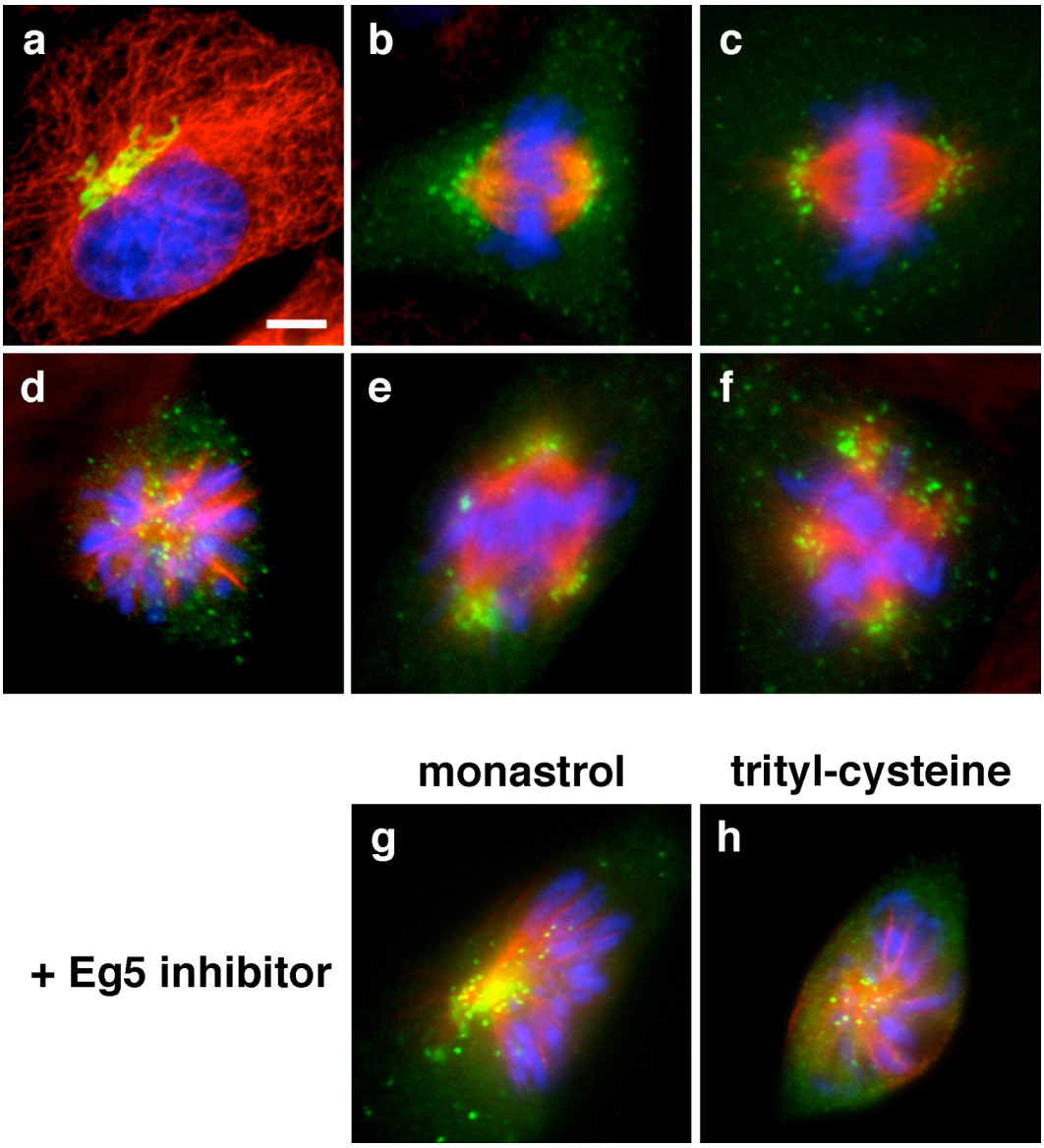

Figure 6. Mitotic Golgi membranes accumulate at the spindle poles. PtK1 cells were stained for the Golgi resident enzyme NAGT I-GFP (a,b) or the Golgi matrix protein GM130 (c-h) (green), tubulin (red) and DNA (blue). Upon entry into mitosis, the Golgi ribbon (a) was disassembled into vesicles that clustered around the spindle poles in metaphase (b,c). Mitotic Golgi membranes concentrated at the spindle poles in cells containing monopolar (d), tripolar (e) or tetrapolar (f) spindles as well as in cells with monopolar spindles induced by an Eg5 inhibitor, either monastrol (g) or trityl-cysteine (h). Bar, 4 μm.

cells and was observed for both the stably-expressed GFP-tagged Golgi enzyme *N*-acetylglucosaminyl transferase I (NAGT I) and the endogenous Golgi matrix protein GM130 (Figure 6b,c). I occasionally observed aberrant monopolar, tripolar and tetrapolar spindles and Golgi membranes clustered at the spindle poles as well (Figure 6d-f). Moreover, accumulation of Golgi at the spindle poles was still evident when PtK1 cells were treated with the Eg5 inhibitor monastrol (Mayer et al., 1999) or trityl-cysteine (Skoufias et al., 2006) to induce monopolar spindles (Figure 6g,h). Taken together, these data suggest a robust association of mitotic Golgi membranes with the spindle apparatus.

To test whether the spindle is required for Golgi partitioning, I established a system where mitotic cells were induced to divide asymmetrically into two daughter cells, only one of which received the entire spindle (Figure 7a). PtK1 cells stably expressing NAGT I-GFP were treated with an Eg5 inhibitor, either monastrol or trityl-cysteine. Upon entry into mitosis, inhibition of the kinesin Eg5 blocks centrosome separation, leading to the formation of monoasters and the arrest of cells in M-phase (Mayer et al., 1999). Monoasters consist of microtubules emanating from non-separated centrosomes and are surrounded by condensed chromosomes. Since PtK1 cells remain relatively flat during mitosis, monoasters are often asymmetrically located at one side of the cells (Canman et al., 2003). I then induced cell division by two independent methods. I microinjected recombinant Mad1 to sequester Mad2 from the kinetochores, which silences the spindle checkpoint and allows progression through mitosis (Canman et al., 2003). I also found that asymmetric cell division could be induced by inhibition of

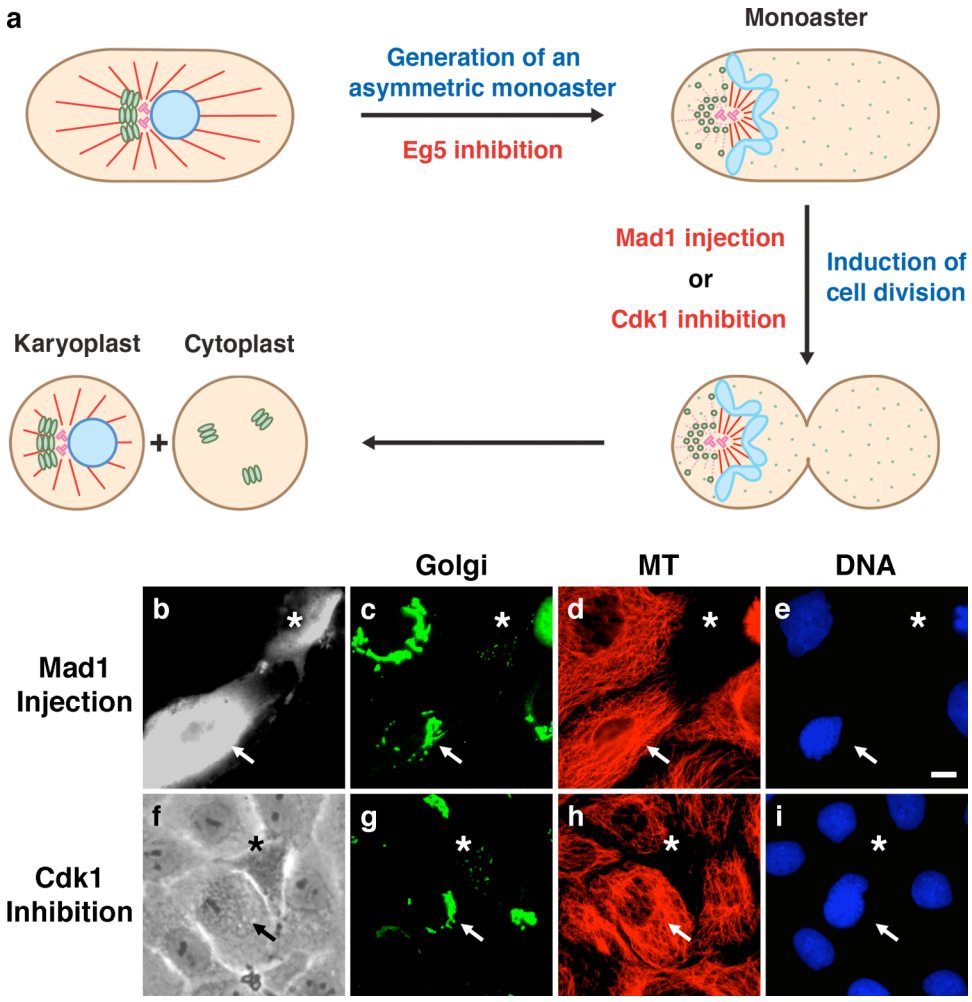

Figure 7. The Golgi in the karyoplasts but not in the cytoplasts reforms a ribbon. (a) Diagram of the assay. PtK1 cells stably expressing NAGT I-GFP were treated with an Eg5 inhibitor (monastrol or trityl-cysteine) for 2 h to induce asymmetrically positioned monoasters. Cell division was then triggered either by microinjection of Mad1 or by addition of a Cdk1 inhibitor (purvalanol A or roscovitine), leading to a karyoplast that received the entire spindle (centrosomes, chromosomes, and spindle microtubules) and a cytoplast that lacked all these. (b-i) Divided cells were either identified by the injection marker (b, Mad1 injection) or followed by time-lapse phase contrast microscopy (f, Cdk1 inhibition). Cells were stained for GFP (c,g), tubulin (d,h) and DNA (e,i). The Golgi in the karyoplasts (↗) reformed a characteristic ribbon in the perinuclear region while the Golgi in the cytoplasts (*) was scattered throughout the cytoplasm (c,g). In addition, no microtubule network was present in the cytoplasts (d,h). Bar, 10 μm.

Cdk1 with roscovitine or purvalanol A (Hu et al., 2008; Niiya et al., 2005). Both approaches generated a cytoplast without a nucleus and a nucleated karyoplast. Daughter cells were either identified by the injection marker (Mad1 injection) or monitored by time-lapse phase contrast microscopy (Cdk1 inhibition).

After division the karyoplasts received the chromosomes (Figure 7e,i), centrosomes (unpublished data) and microtubules (Figure 7d,h), whereas the cytoplasts lacked all of these. Intriguingly, Golgi markers, including NAGT I-GFP and GM130, were detected in both cells (Figure 7c,g), suggesting that parts of the Golgi were partitioned independently of the spindle (n=29 for Mad1 injection and n>50 for Cdk1 inhibition). However, the organization of the Golgi in the two daughter cells was very different. I analyzed the Golgi distribution in each daughter cell where the Golgi was determined as a ribbon if 90% of the fluorescence resided in no more than three continuous structures (Puthenveedu et al., 2006). The Golgi in the karyoplasts localized to the perinuclear region and exhibited the characteristic ribbon structure (Figure 7c,g). By contrast, the Golgi in the cytoplasts was spread throughout the cytoplasm and failed to reform a ribbon (Figure 7c,g). This indicates that the spindle has a direct role in inheritance of the Golgi ribbon.

To eliminate the possibility that the scattered Golgi in the cytoplasts might be due to cell death, I followed both karyoplasts and cytoplasts by video microscopy. The cytoplasts survived on average 36 h after division and, in some cases, were still alive and seemingly healthy when corresponding karyoplasts underwent a second round of cell division.

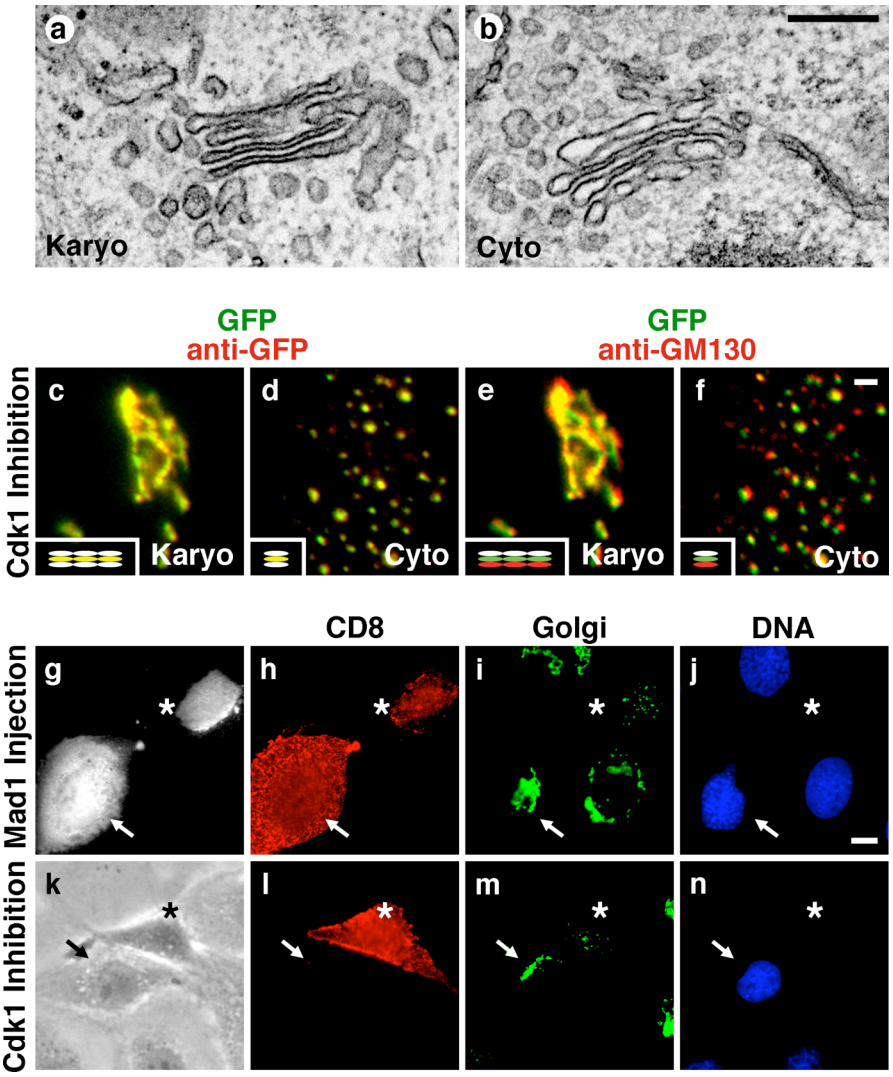

Figure 8. The Golgi stacks in the cytoplasts are polarized and transport cargo. (a-f) The Golgi in the cytoplasts is composed of polarized stacks. PtK1 cells stably expressing the *medial/trans*-Golgi enzyme NAGT I-GFP were induced to divide asymmetrically and followed by video microscopy. Upon division, cells were either processed for EM (a,b) or for immunofluorescence (c-f). (a,b) Stacked Golgi cisternae reformed in both karyoplasts (a) and cytoplasts (b). Bar, 200 nm. (c-f) The Golgi stacks are polarized. Divided cells were triple-labeled with GFP, anti-GFP and anti-*cis*-Golgi marker GM130. Two-channel overlays were performed as specified. GFP fluorescence is shown in green (c-f) and the antibody stainings for GFP (c,d) and GM130 (e,f) are pseudo-colored in red. The GFP fluorescence colocalized with the anti-GFP signal (c,d), but only partially overlapped with

The scattered Golgi and the absence of microtubules in the cytoplasts are reminiscent of cells treated with nocodazole, which causes the Golgi ribbon to fragment into stacks that are dispersed throughout the cell (Shima et al., 1998). Our EM analysis revealed that the Golgi in both karyoplasts and cytoplasts was stacked with an average of 3.4 ± 0.7 (karyoplast, n=22) and 3.3 ± 0.6 (cytoplast, n=23) cisternae per stack (Figure 8a,b). The cisternae were stacked to a comparable extent and separated by 11.8 ± 3.8 nm (karyoplast) and 12.9 ± 3.7 nm (cytoplast). To determine whether the stacks are polarized, I took advantage of a well-established fluorescence microscopy method (Shima et al., 1997). PtK1 cells stably expressing the *medial/trans*-Golgi enzyme NAGT I-GFP were induced to divide asymmetrically and then immunolabeled for GFP and the *cis*-Golgi marker GM130 (n=15). In these triple-labeled cells, the GFP fluorescence was overlaid with the anti-GFP and anti-GM130 signals respectively. The anti-GFP staining served as a control showing a complete overlap with the GFP fluorescence (Figure 8c,d). In contrast, the *cis* anti-GM130 signal in the karyoplasts was found adjacent to the *medial/trans* GFP fluorescence with only a partial overlap (Figure 8e), suggesting that the ribbon in the karyoplasts preserved a *cis*-to-*trans* polarity. A similar segregation pattern was observed in the cytoplasts (Figure 8f). Together with our EM data, I conclude that the scattered Golgi in the cytoplasts is stacked and polarized.

(**Figure 8.** continued) the anti-GM130 signal (e,f) in both karyoplasts (c,e) and cytoplasts (d,f), as shown schematically in the insets. Bar, 2 μm. (g-n) CD8 transport assay. CD8 mRNA was microinjected into cells with asymmetric monoasters together with Mad1 (g-j) or into the cytoplasts induced by Cdk1 inhibition (k-n). CD8 on the cell surface was stained before permeabilization (h,l). Note that CD8 was expressed and transported to the plasma membrane in the cytoplasts (*). Karyoplasts are marked by arrows (↗). Bar, 10 μm.

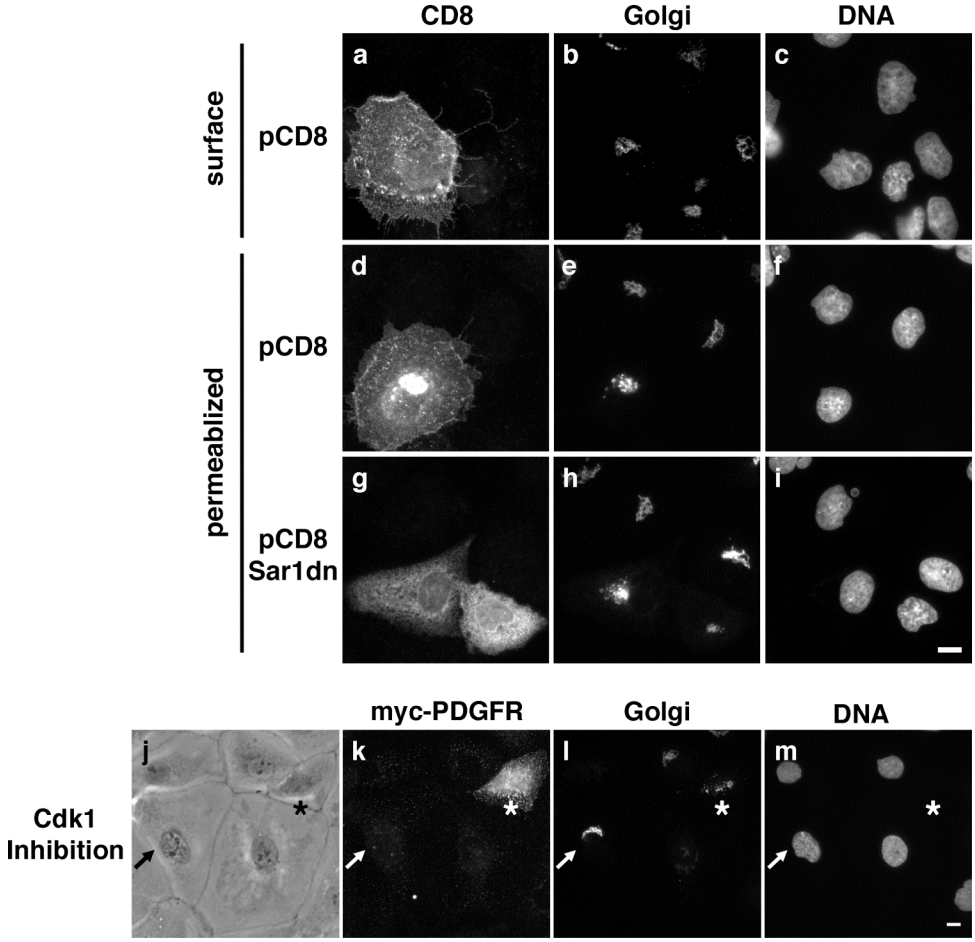

Figure 9. Transport of newly synthesized proteins to the cell surface. (a-i) PtK1 cells stably expressing NAGT I-GFP were microinjected with a plasmid encoding CD8 alone (a-f) or together with Sar1dn protein (g-i). After 3 h expression, cells were labeled for CD8 on the cell surface without permeabilization (a-c) or fixed and permeabilized before staining for CD8 (d-i). The Golgi was visualized by GFP and DNA was stained with Hoechst. (a-c) CD8 was detected on the cell surface of non-permeabilized cells. (d-f) In permeabilized cells, CD8 was detected in the Golgi in addition to the plasma membrane. (g-i) Sar1dn blocked transport to the cell surface and CD8 was retained in the ER. (j-m) Secretion is functional in the cytoplasts. Asymmetric cell division was induced by Cdk1 inhibition and followed by video microscopy (j). The cytoplasts were then microinjected with the mRNA of myc-tagged protein A fused to the transmembrane domain of the PDGF receptor. After 2 h expression, cells were stained for myc without permeabilization. Cytoplasts are marked by asterisks and the arrows point at karyoplasts. Note that myc-PDGFR was transported to the plasma membrane. Bar, 10 μm.

I next investigated whether the stacked Golgi in the cytoplasts transports cargo. The mRNA of CD8, a plasma membrane protein not expressed in PtK1 cells, was injected together with Mad1 protein into cells with asymmetric monoasters. Cells were incubated for 4 h to allow cell division as well as synthesis and transport of cargo, then fixed and stained before permeabilization. CD8 was detected on the cell surface in both karyoplasts and cytoplasts (Figure 8h; n=22), but not in cells with impaired secretion (Figure 9), indicating that the Golgi stacks in both cells transported cargo. To rule out that CD8 might have been expressed and transported before cytokinesis, I induced asymmetric cell division in the presence of the protein synthesis inhibitor cycloheximide. After the drug was removed to allow protein expression and transport, CD8 was detected on the cell surface of both cells (unpublished data; n=9). In another approach, I injected CD8 mRNA into the cytoplasts generated by Cdk1 inhibition. CD8 appeared on the cell surface of the cytoplasts but not on the non-injected karyoplasts (Figure 8l; n=8). Similarly, myc-tagged protein A fused to the transmembrane domain of the PDGF receptor was also delivered to the cell surface (Figure 9k; n=15). These findings indicate that the Golgi stacks in the cytoplasts are functional for secretion and do not require the spindle for partitioning.

In principle, the lack of a Golgi ribbon in the cytoplasts could be explained by two different mechanisms. First, the failure in ribbon assembly might be due to the absence of microtubules in the cytoplasts, since microtubules are essential to establish a Golgi ribbon. In this case, reformation of microtubules should restore the ribbon. Alternatively, the scattered Golgi stacks in the cytoplasts might be caused by the exclusion of the

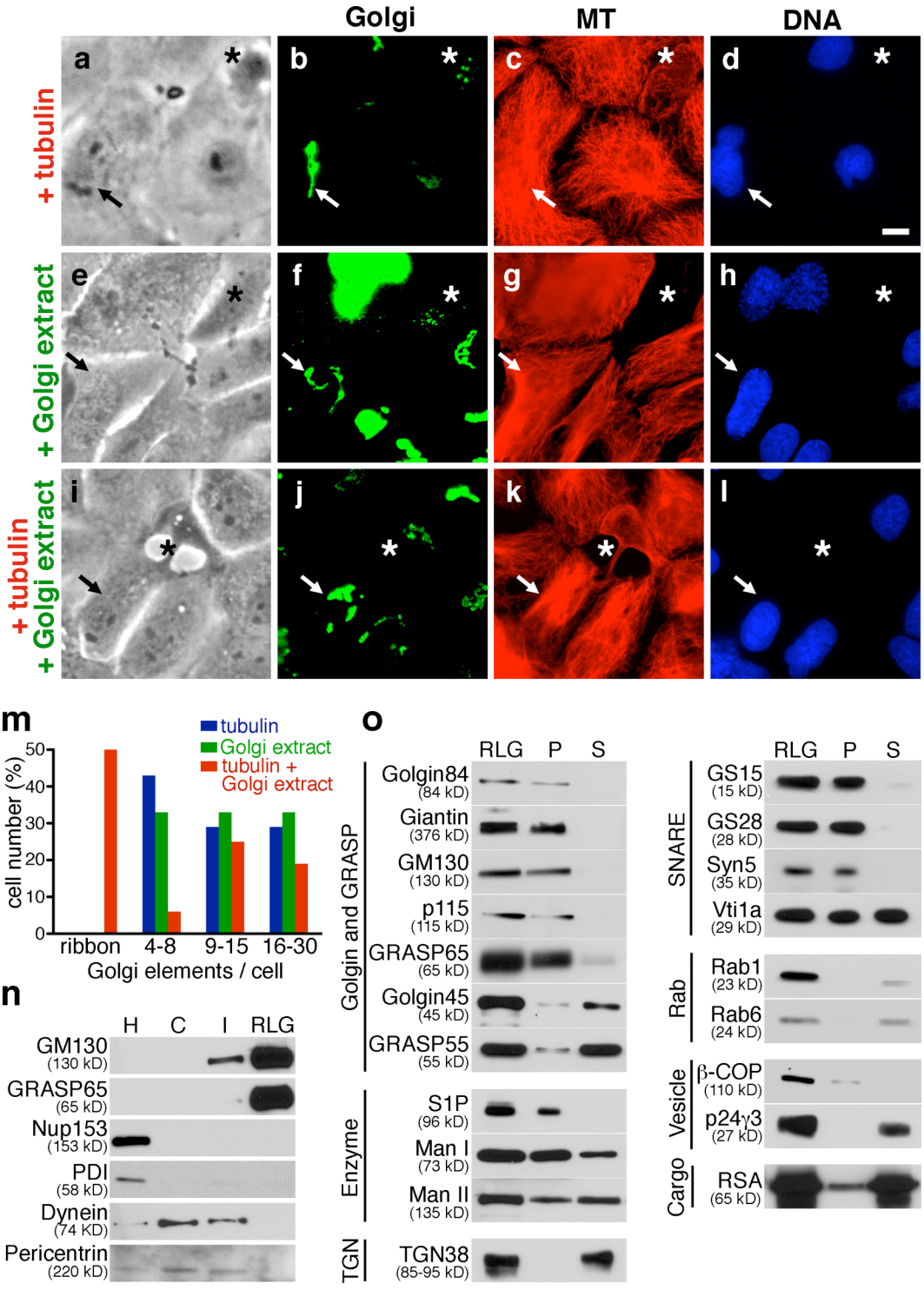
Golgi
MT
DNA
+ tubulin
+ Golgi extract
+ tubulin
+ Golgi extract
a
b
c
d
e
f
g
h
i
j
k
l
m
tubulin
Golgi extract
tubulin + Golgi extract
cell number (%)
50
40
30
20
10
0
ribbon
4-8
9-15
16-30
Golgi elements / cell
n
H
C
I
RLG
GM130 (130 kD)
GRASP65 (65 kD)
Nup153 (153 kD)
PDI (58 kD)
Dynein (74 KD)
Pericentrin (220 kD)
o
RLG
P
S
Golgin and GRASP
Golgin84 (84 kD)
Giantin (376 kD)
GM130 (130 kD)
p115 (115 kD)
GRASP65 (65 kD)
Golgin45 (45 kD)
GRASP55 (55 kD)
Enzyme
S1P (96 kD)
Man I (73 kD)
Man II (135 kD)
TGN
TGN38 (85-95 kD)
SNARE
GS15 (15 kD)
GS28 (28 kD)
Syn5 (35 kD)
Vti1a (29 kD)
Rab
Rab1 (23 kD)
Rab6 (24 kD)
Vesicle
β-COP (110 kD)
p24γ3 (27 kD)
Cargo
RSA (65 kD)

factors required for ribbon assembly (i.e. ribbon determinants). Ribbon determinants may associate with the spindle and are therefore not transferred to the cytoplasts. Supplying these factors should rescue ribbon formation. To distinguish between these two possibilities, I injected the missing materials into the cytoplasts and examined the Golgi morphology. Injection of tubulin resulted in a microtubule network (Figure 10c), demonstrating that the cellular environment in the cytoplasts supports microtubule polymerization (Pelletier et al., 2000). The overall organization of Golgi stacks, however, remained scattered (Figure 10b; n=14; 5 independent experiments), indicating that the microtubules in the cytoplasts are not sufficient to reassemble a ribbon. Therefore, additional factors might be required but presumably were segregated along with the spindle into the karyoplasts. Since these factors may associate with Golgi membranes, I

Figure 10. Ribbon determinants are localized to the Golgi. Rescue of the ribbon by coinjection of Golgi extract with tubulin. Tubulin alone (a-d), or Golgi extract without (e-h) or with tubulin (i-l) were microinjected into the cytoplasts (*). After 2 h incubation, cells were stained for GFP (b,f,j), tubulin (c,g,k) and DNA (d,h,l). Injection of tubulin or Golgi extract alone had no effect (b*,f*), whereas Golgi extract together with tubulin reconstituted a Golgi ribbon (j*). Karyoplasts are marked by arrows (↗). Bar, 10 μm. (m) Distribution of Golgi elements in the injected cytoplasts. A ribbon is formed if the Golgi is in no more than 3 continuous structures. (n) Equal amounts of protein (4 μg) of rat liver homogenate (H), cytosol (C), intermediate fraction (I) and Golgi membranes (RLG) were immunoblotted for the Golgi proteins GM130 and GRASP65, nuclear pore complex protein Nup153, ER enzyme PDI, motor protein dynein and centrosome marker pericentrin. GM130 and GRASP65 were highly enriched on RLG membranes, while Nup153, PDI, dynein and pericentrin were not detectable. (o) *Medial/trans*-Golgi proteins are enriched in the detergent extract. RLG membranes were extracted with n-octylglucoside, cleared by centrifugation (pellet, P) and the supernatant was dialyzed to remove the detergent (S). Equal volumes of each fraction were immunoblotted for the indicated proteins. *Cis*-Golgi proteins were de-enriched (e.g. Golgin84, GM130, GRASP65), while markers of the *medial/trans*-Golgi and the TGN were enriched in the extract (e.g. Golgin45, GRASP55, Vti1a, TGN38).

extracted rat liver Golgi (RLG) membranes with the non-ionic detergent *n*-octylglucoside and then removed the detergent by dialysis. Injection of Golgi extract alone had no effect (Figure 10f; n=12; 4 independent experiments), but Golgi extract together with tubulin restored a ribbon (Figure 10j; n=8; 5 independent experiments) as well as a microtubule network (Figure 10k). Thus, the factors required for ribbon assembly are located on the Golgi.

This is in line with previous studies showing that in cytoplasts generated by microsurgery, a Golgi ribbon forms in the absence of centrosomes but requires pre-existing Golgi distributed into the cut cells under interphase condition (Maniotis and Schliwa, 1991; Pelletier et al., 2000). The mammalian Golgi ribbon is usually formed next to the centrosomes, which depends on the minus end-directed microtubule motor dynein. I did not detect centrosomes in serial sections of RLG membranes by EM. In addition, neither the centrosomal marker pericentrin nor cytoplasmic dynein were detectable by western blotting in the RLG fraction, although the proteins were present in the homogenate (Figure 10n). Similarly, the ER enzyme PDI and the nuclear pore protein Nup153 were absent in the RLG fraction. In contrast, the Golgi proteins GM130 and GRASP65 were highly enriched. Interestingly, I found *medial/trans*-Golgi markers were enriched in the Golgi extract, while *cis*-Golgi proteins were mostly depleted (Figure 10o). This implies that the factors required for post-mitotic ribbon reassembly might have distinct molecular compositions from the *cis*-Golgi proteins Golgin84, GRASP65 and GM130 shown to be required for ribbon maintenance in interphase (Diao et al., 2003; Puthenveedu et al., 2006).

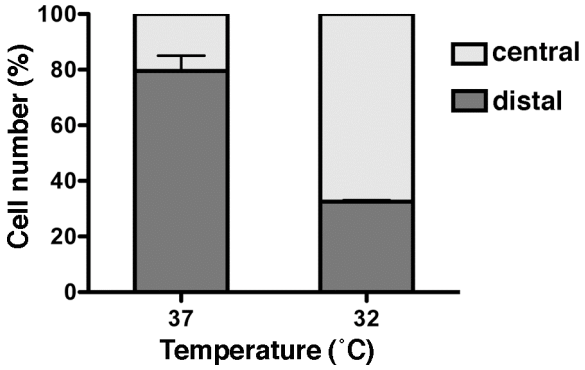

Figure 11. Temperature affects spindle positioning during division. Unsynchronized PtK1 cells were treated with trityl-cysteine for 2 h. Cell division was then followed by time-lapse phase contrast microscopy after addition of purvalanol A. In cells that entered mitosis at 37ºC, the monopolar spindle was positioned distal to the cleavage furrow. At 32ºC, the spindle was positioned centrally in close proximity to the cell division plane. For each experiment, 285 non-overlapping microscopic fields were monitored to ensure unbiased sampling. Error bars represent standard error of the mean from two independent experiments with an average of 50 cells per condition.

If the ribbon determinants are partitioned with the spindle, then incorporation of parts of the spindle and its associated proteins into the cytoplasts should rescue ribbon formation. I followed asymmetric cell division induced at lower temperature (32ºC) and found that spindle positioning was dramatically altered, presumably caused by effects on microtubule dynamics (Figure 11). At 37ºC, the monopolar spindle was positioned distal to the cleavage furrow and seemingly adhered to the cortex at one side of the cell (Figure 12a). The cytoplasts derived from this type of division contained scattered Golgi but no microtubules as described above (Figures 7g,h and 12b,c). At lower temperature, however, the spindle was positioned centrally in close proximity to the division plane (Figure 12e), which allowed partial incorporation of spindle materials into the cytoplasts,

as revealed by the presence of a microtubule network (Figure 12g). Furthermore, a Golgi ribbon reformed (Figure 12f; n=21), suggesting that ribbon determinants were segregated into the cytoplasts. Therefore, these data support the idea that ribbon factors are bound to and partitioned together with the spindle.

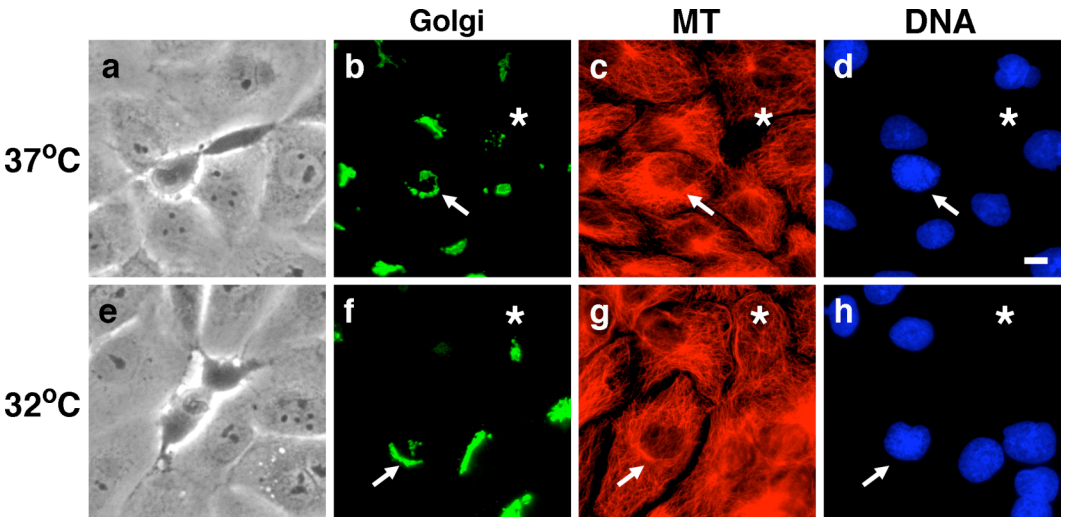

Figure 12. Ribbon determinants partition together with the spindle. Rescue of the ribbon by incorporation of spindle materials. Cells induced to divide asymmetrically at 37°C (a-d) or 32°C (e-h) were followed by video microscopy, and then stained for GFP (b,f), tubulin (c,g) and DNA (d,h). At 37°C, the spindle was located distal to the division plane (a). Microtubules were not partitioned into the cytoplasts (c*) and the Golgi was scattered (b*). At 32°C, the spindle was positioned close to the cleavage furrow (e). Spindle microtubules were incorporated into the cytoplasts (g*) and a Golgi ribbon reformed (f*). Karyoplasts are marked by arrows (↗). Bar, 10 μm.

3. Discussion

In metaphase, Golgi membranes decorate the spindle poles, suggesting that the spindle might regulate Golgi partitioning (Jokitalo et al., 2001). By uncoupling cytokinesis from chromosome segregation, I have demonstrated that the spindle directly partitions the factors required for Golgi ribbon assembly, thus extending the role of the spindle beyond chromosome segregation. In addition, our approach provides a potential avenue for investigating the nature of cytoplasm *in vivo* and free from the influence of the nucleus. In our case, the cytoplasts contained all the machinery required for protein synthesis (i.e. ribosomes) and exocytosis (i.e. ER and Golgi).

The cytoplasts received Golgi stacks capable of secretion independently of the spindle, but these stacks were not linked into a ribbon. This is in contrast to the karyoplasts where a ribbon reformed. Taken together, our data suggest two distinct mechanisms underlying Golgi inheritance. First, minimum functional Golgi units (stacks) are inherited in a spindle-independent manner. These stacks could be derived from Golgi that was partitioned together with the ER (Zaal et al., 1999), or could have reassembled from the Golgi that was segregated independently of the spindle (Jesch et al., 2001b). Second, the mitotic spindle plays a vital role in transmitting ribbon determinants into the daughter cells.

The appearance of the Golgi ribbon in higher organisms during evolution reflects a different mechanism for polarized secretion. In lower animals such as *Drosophila*, Golgi

stacks are scattered and localized adjacent to ER exit sites despite the presence of centrosomes. Polarized secretion is achieved by targeting mRNA to specific ER exit sites where the cargo is made and secreted locally (Herpers and Rabouille, 2004). In mammalian cells, however, cargo is post-translationally sorted from the centrally located Golgi ribbon (for review, see (Bard and Malhotra, 2006). To establish cell polarity, the entire Golgi ribbon is reoriented towards the site of secretion (Bisel et al., 2008), which is essential for a variety of cellular processes, such as the outgrowth of dendrites in neurons (Horton et al., 2005), fibroblast migration during wound healing (Preisinger et al., 2004), and the immune response (Stinchcombe et al., 2006). Since the ribbon is particularly important for more advanced functions, tight coupling of ribbon determinants with the spindle ensures that each daughter cell receives the information to assemble it. This might be the reason that mammalian cells employ the highly regulated spindle apparatus to partition these factors instead of a stochastic ER-dependent process.

Chapter Four Conclusions

Like all other cellular organelles, the Golgi apparatus grows in interphase and is divided into the daughter cells in mitosis. During cell division, the single continuous Golgi ribbon in mammalian cells is disassembled in early mitosis and reformed upon partitioning in both daughter cells (Lowe and Barr, 2007; Shorter and Warren, 2002). The nuclear envelope is also dissolved at the onset of mitosis to allow chromosome segregation. For the purpose of partitioning, the nuclear membranes are first absorbed into the ER and re-emerge out of the ER at the end of mitosis to assemble a nuclear envelope around the decondensing chromosomes (Ellenberg et al., 1997; Yang et al., 1997). The Golgi has been suggested to follow the same fate as the nuclear envelope during mitosis, where the disassembled Golgi membranes fuse with the ER (Altan-Bonnet et al., 2006; Zaal et al., 1999). However, several recent reports presented compelling evidence against this mode of partitioning. Instead of merging with the ER, the Golgi membranes remain distinct and separated from the ER throughout mitosis (Axelsson and Warren, 2004; Bartz and Seemann, 2008; Jesch et al., 2001b; Pecot and Malhotra, 2004). The mitotic spindle instead has been proposed to play a key role in the Golgi division process, based on two major observations. First, Golgi partitioning is highly accurate to a comparable extent as chromosome segregation that utilizes the spindle machinery (Seemann et al., 2002; Shima et al., 1997). Second, mitotic Golgi membranes are found concentrated around the two spindle poles (Bartz et al., 2008; Shima et al., 1998). Whether the spindle is indeed involved in organizing Golgi division was so far difficult to analyze, because Golgi segregation could not be uncoupled from chromosome and centrosome separation.

To dissect the function of the spindle in Golgi partitioning, I recently established an approach by which cytokinesis proceeds in the absence of chromosome segregation (Wei and Seemann, 2009). By overriding the spindle checkpoint and triggering cytokinesis, this assay allows to directly test whether the mitotic spindle is necessary for Golgi inheritance. Cells are first treated with the Eg5 inhibitor (monastrol or trityl cysteine) that blocks centrosome separation in prophase. As a result, the cells become arrested in early mitosis with monopolar spindles (Mayer et al., 1999). The disassembled Golgi membranes in these cells behave similarly to those in untreated cells and still accumulate around the poles of the monopolar spindles. To induce cell division, the spindle checkpoint is then bypassed by microinjection of Mad1 recombinant protein (Canman et al., 2003) or by addition of a Cdk1 inhibitor such as roscovitine or purvalanol A (Hu et al., 2008; Niiya et al., 2005). Subsequently the cells assemble a cleavage furrow and complete cytokinesis, which gives rise to a karyoplast that receives the entire spindle, chromosomes and centrosomes, and a cytoplast lacking all of these.

In the karyoplast, Golgi stacks reassemble and are laterally linked together into one continuous ribbon in the perinuclear region. In the cytoplast, stacked and polarized Golgi cisternae also reform, which are fully functional in transporting cargo through the secretory pathway. In contrast to the karyoplast, however, these stacks are scattered throughout the cytoplasm and not interconnected into a ribbon. This suggests that the factors required for ribbon formation are partitioned together with the spindle and are therefore not present in the cytoplast. Indeed, by lowering the division temperature, the spindle is positioned closer to the cleavage furrow, which allows some spindle

microtubules with associated membranes, but not chromosomes, to be incorporated into the cytoplast. The resulting cytoplast reforms an intact Golgi ribbon, demonstrating that the factors required for ribbon assembly are linked to the spindle. Alternatively, a ribbon can be restored by adding back the missing factors to the cytoplast. Microinjection of a Golgi detergent extract together with tubulin into the cytoplast fully reestablishes a Golgi ribbon. These findings uncover that Golgi partitioning is regulated by two distinct mechanisms. Polarized stacks of Golgi cisternae, the basic units functional in secretion, are segregated into progeny by a spindle-independent process. In contrast, the factors that link the stacks into a continuous ribbon are partitioned together with the spindle.

Previous reports demonstrated that downregulation of the *cis*-Golgi matrix proteins GM130 and GRASP65 by RNAi disrupts the Golgi ribbon structure (Puthenveedu et al., 2006), suggesting that the two proteins might play a role in lateral linkage of Golgi stacks into a ribbon under the interphase condition. However, we observed that both GM130 and GRASP65 are present in the cytoplast, indicating that neither GM130 nor GRASP65 is sufficient to reform a Golgi ribbon, at least in post-mitotic cells. Furthermore, upon microinjection of the mRNAs of GM130 and GRASP65 together with purified tubulin into the cytoplast, both proteins are expressed, but a ribbon is not formed and individual Golgi stacks remain scattered. Interestingly, expression of GM130 and GRASP65 causes extensive tubulation of the scattered Golgi stacks. Tubular profiles positive for GM130 have been described to carry cargo proteins between the peripheral intermediate compartment and the centrally located Golgi ribbon (Marra et al., 2001), but the structures I observed were more prominent and numerous. The tubulation may reflect an

initial step in mobilizing the Golgi stacks along microtubule tracks. If other parts of the Golgi remain static, only tubules are pulled out of the Golgi membranes and the Golgi elements are not brought together.

In addition, the microinjected protein extract that rescues ribbon assembly is depleted of both GM130 and GRASP65 and instead enriched in proteins resident to *medial/trans*-cisternae. In fact, the majority of *cis*-Golgi proteins are either absent or highly de-enriched in this extract. Therefore, *medial/trans*-Golgi proteins contain the information to restore the ribbon. Taken together, our data suggest that post-mitotic ribbon formation depends on a different subset of Golgi proteins (*medial/trans* proteins) rather than those required for the maintenance of the ribbon in interphase.

BIBLIOGRAPHY

Altan-Bonnet, N., Phair, R.D., Polishchuk, R.S., Weigert, R., and Lippincott-Schwartz, J. (2003). A role for Arf1 in mitotic Golgi disassembly, chromosome segregation, and cytokinesis. Proceedings of the National Academy of Sciences of the United States of America *100*, 13314-13319.

Altan-Bonnet, N., Sougrat, R., Liu, W., Snapp, E.L., Ward, T., and Lippincott-Schwartz, J. (2006). Golgi inheritance in mammalian cells is mediated through endoplasmic reticulum export activities. Mol Biol Cell *17*, 990-1005.

Axelsson, M.A., and Warren, G. (2004). Rapid, endoplasmic reticulum-independent diffusion of the mitotic Golgi haze. Mol Biol Cell *15*, 1843-1852.

Bard, F., and Malhotra, V. (2006). The formation of TGN-to-plasma-membrane transport carriers. Annu Rev Cell Dev Biol *22*, 439-455.

Barr, F.A., Puype, M., Vandekerckhove, J., and Warren, G. (1997). GRASP65, a protein involved in the stacking of Golgi cisternae. Cell *91*, 253-262.

Bartz, R., and Seemann, J. (2008). Mitotic regulation of SREBP and ATF6 by separation of the Golgi and ER. Cell cycle *7*, 2100-2105.

Bartz, R., Sun, L.P., Bisel, B., Wei, J.H., and Seemann, J. (2008). Spatial separation of Golgi and ER during mitosis protects SREBP from unregulated activation. Embo J *27*, 948-955.

Beard, M., Satoh, A., Shorter, J., and Warren, G. (2005). A cryptic Rab1-binding site in the p115 tethering protein. J Biol Chem *280*, 25840-25848.

Bisel, B., Wang, Y., Wei, J.H., Xiang, Y., Tang, D., Miron-Mendoza, M., Yoshimura, S., Nakamura, N., and Seemann, J. (2008). ERK regulates Golgi and centrosome orientation towards the leading edge through GRASP65. J Cell Biol *182*, 837-843.

Canman, J.C., Cameron, L.A., Maddox, P.S., Straight, A., Tirnauer, J.S., Mitchison, T.J., Fang, G., Kapoor, T.M., and Salmon, E.D. (2003). Determining the position of the cell division plane. Nature *424*, 1074-1078.

Canman, J.C., Sharma, N., Straight, A., Shannon, K.B., Fang, G., and Salmon, E.D. (2002). Anaphase onset does not require the microtubule-dependent depletion of kinetochore and centromere-binding proteins. J Cell Sci *115*, 3787-3795.

Colanzi, A., Hidalgo Carcedo, C., Persico, A., Cericola, C., Turacchio, G., Bonazzi, M., Luini, A., and Corda, D. (2007). The Golgi mitotic checkpoint is controlled by

BARS-dependent fission of the Golgi ribbon into separate stacks in G2. EMBO J *26*, 2465-2476.

Cole, N.B., Sciaky, N., Marotta, A., Song, J., and Lippincott-Schwartz, J. (1996). Golgi dispersal during microtubule disruption: regeneration of Golgi stacks at peripheral endoplasmic reticulum exit sites. Mol Biol Cell *7*, 631-650.

Corda, D., Colanzi, A., and Luini, A. (2006). The multiple activities of CtBP/BARS proteins: the Golgi view. Trends In Cell Biology *16*, 167-173.

DeBose-Boyd, R.A., Brown, M.S., Li, W.P., Nohturfft, A., Goldstein, J.L., and Espenshade, P.J. (1999). Transport-dependent proteolysis of SREBP: relocation of site-1 protease from Golgi to ER obviates the need for SREBP transport to Golgi. Cell *99*, 703-712.

Diao, A., Frost, L., Morohashi, Y., and Lowe, M. (2008). Coordination of golgin tethering and SNARE assembly: GM130 binds syntaxin 5 in a p115-regulated manner. J Biol Chem *283*, 6957-6967.

Diao, A., Rahman, D., Pappin, D.J., Lucocq, J., and Lowe, M. (2003). The coiled-coil membrane protein golgin-84 is a novel rab effector required for Golgi ribbon formation. J Cell Biol *160*, 201-212.

Draviam, V.M., Orrechia, S., Lowe, M., Pardi, R., and Pines, J. (2001). The localization of human cyclins B1 and B2 determines CDK1 substrate specificity and neither enzyme requires MEK to disassemble the Golgi apparatus. J Cell Biol *152*, 945-958.

Duran, J.M., Kinseth, M., Bossard, C., Rose, D.W., Polishchuk, R., Wu, C.C., Yates, J., Zimmerman, T., and Malhotra, V. (2008). The role of GRASP55 in Golgi fragmentation and entry of cells into mitosis. Mol Biol Cell *19*, 2579-2587.

Ellenberg, J., Siggia, E.D., Moreira, J.E., Smith, C.L., Presley, J.F., Worman, H.J., and Lippincott-Schwartz, J. (1997). Nuclear membrane dynamics and reassembly in living cells: targeting of an inner nuclear membrane protein in interphase and mitosis. J Cell Biol *138*, 1193-1206.

Farkas, R.M., Giansanti, M.G., Gatti, M., and Fuller, M.T. (2003). The Drosophila Cog5 homologue is required for cytokinesis, cell elongation, and assembly of specialized Golgi architecture during spermatogenesis. Mol Biol Cell *14*, 190-200.

Feinstein, T.N., and Linstedt, A.D. (2007). Mitogen-activated protein kinase kinase 1-dependent Golgi unlinking occurs in G2 phase and promotes the G2/M cell cycle transition. Mol Biol Cell *18*, 594-604.

Gaietta, G.M., Giepmans, B.N., Deerinck, T.J., Smith, W.B., Ngan, L., Llopis, J., Adams, S.R., Tsien, R.Y., and Ellisman, M.H. (2006). Golgi twins in late mitosis revealed by genetically encoded tags for live cell imaging and correlated electron microscopy. Proceedings of the National Academy of Sciences of the United States of America *103*, 17777-17782.

Gallop, J.L., Butler, P.J., and McMahon, H.T. (2005). Endophilin and CtBP/BARS are not acyl transferases in endocytosis or Golgi fission. Nature *438*, 675-678.

Glotzer, M. (2001). Animal cell cytokinesis. Annu Rev Cell Dev Biol *17*, 351-386.

Goss, J.W., and Toomre, D.K. (2008). Both daughter cells traffic and exocytose membrane at the cleavage furrow during mammalian cytokinesis. J Cell Biol *181*, 1047-1054.

Gromley, A., Yeaman, C., Rosa, J., Redick, S., Chen, C.T., Mirabelle, S., Guha, M., Sillibourne, J., and Doxsey, S.J. (2005). Centriolin anchoring of exocyst and SNARE complexes at the midbody is required for secretory-vesicle-mediated abscission. Cell *123*, 75-87.

Hammond, C., and Helenius, A. (1994). Quality control in the secretory pathway: retention of a misfolded viral membrane glycoprotein involves cycling between the ER, intermediate compartment, and Golgi apparatus. J Cell Biol *126*, 41-52.

He, C.Y. (2007). Golgi biogenesis in simple eukaryotes. Cell Microbiol *9*, 566-572.

Herpers, B., and Rabouille, C. (2004). mRNA localization and ER-based protein sorting mechanisms dictate the use of transitional endoplasmic reticulum-golgi units involved in gurken transport in Drosophila oocytes. Mol Biol Cell *15*, 5306-5317.

Hidalgo Carcedo, C., Bonazzi, M., Spano, S., Turacchio, G., Colanzi, A., Luini, A., and Corda, D. (2004). Mitotic Golgi partitioning is driven by the membrane-fissioning protein CtBP3/BARS. Science *305*, 93-96.

Horton, A.C., Rácz, B., Monson, E.E., Lin, A.L., Weinberg, R.J., and Ehlers, M.D. (2005). Polarized secretory trafficking directs cargo for asymmetric dendrite growth and morphogenesis. Neuron *48*, 757-771.

Hu, C.K., Coughlin, M., Field, C.M., and Mitchison, T.J. (2008). Cell polarization during monopolar cytokinesis. J Cell Biol *181*, 195-202.

Jesch, S.A., Lewis, T.S., Ahn, N.G., and Linstedt, A.D. (2001a). Mitotic phosphorylation of Golgi reassembly stacking protein 55 by mitogen-activated protein kinase ERK2. Mol Biol Cell *12*, 1811-1817.

Jesch, S.A., Mehta, A.J., Velliste, M., Murphy, R.F., and Linstedt, A.D. (2001b). Mitotic Golgi is in a dynamic equilibrium between clustered and free vesicles independent of the ER. Traffic *2*, 873-884.

Jokitalo, E., Cabrera-Poch, N., Warren, G., and Shima, D.T. (2001). Golgi clusters and vesicles mediate mitotic inheritance independently of the endoplasmic reticulum. J Cell Biol *154*, 317-330.

Jurgens, G. (2005). Plant cytokinesis: fission by fusion. Trends In Cell Biology *15*, 277-283.

Kano, F., Tanaka, A.R., Yamauchi, S., Kondo, H., and Murata, M. (2004). Cdc2 kinase-dependent disassembly of endoplasmic reticulum (ER) exit sites inhibits ER-to-Golgi vesicular transport during mitosis. Mol Biol Cell *15*, 4289-4298.

Kim, P.K., Mullen, R.T., Schumann, U., and Lippincott-Schwartz, J. (2006). The origin and maintenance of mammalian peroxisomes involves a de novo PEX16-dependent pathway from the ER. J Cell Biol *173*, 521-532.

Ladinsky, M.S., Mastronarde, D.N., McIntosh, J.R., Howell, K.E., and Staehelin, L.A. (1999). Golgi structure in three dimensions: functional insights from the normal rat kidney cell. J Cell Biol *144*, 1135-1149.

Lazarides, E., and Weber, K. (1974). Actin antibody: the specific visualization of actin filaments in non-muscle cells. Proceedings of the National Academy of Sciences of the United States of America *71*, 2268-2272.

Lin, C.Y., Madsen, M.L., Yarm, F.R., Jang, Y.J., Liu, X., and Erikson, R.L. (2000). Peripheral Golgi protein GRASP65 is a target of mitotic polo-like kinase (Plk) and Cdc2. Proceedings of the National Academy of Sciences of the United States of America *97*, 12589-12594.

Litvak, V., Argov, R., Dahan, N., Ramachandran, S., Amarilio, R., Shainskaya, A., and Lev, S. (2004). Mitotic phosphorylation of the peripheral Golgi protein Nir2 by Cdk1 provides a docking mechanism for Plk1 and affects cytokinesis completion. Mol Cell *14*, 319-330.

Lowe, M., and Barr, F.A. (2007). Inheritance and biogenesis of organelles in the secretory pathway. Nat Rev Mol Cell Biol *8*, 429-439.

Lowe, M., Gonatas, N.K., and Warren, G. (2000). The mitotic phosphorylation cycle of the cis-Golgi matrix protein GM130. J Cell Biol *149*, 341-356.

Lowe, M., Rabouille, C., Nakamura, N., Watson, R., Jackman, M., Jamsa, E., Rahman, D., Pappin, D.J., and Warren, G. (1998). Cdc2 kinase directly phosphorylates the

cis-Golgi matrix protein GM130 and is required for Golgi fragmentation in mitosis. Cell *94*, 783-793.

Maniotis, A., and Schliwa, M. (1991). Microsurgical removal of centrosomes blocks cell reproduction and centriole generation in BSC-1 cells. Cell *67*, 495-504.

Marra, P., Maffucci, T., Daniele, T., Tullio, G.D., Ikehara, Y., Chan, E.K., Luini, A., Beznoussenko, G., Mironov, A., and De Matteis, M.A. (2001). The GM130 and GRASP65 Golgi proteins cycle through and define a subdomain of the intermediate compartment. Nat Cell Biol *3*, 1101-1113.

Mayer, T.U., Kapoor, T.M., Haggarty, S.J., King, R.W., Schreiber, S.L., and Mitchison, T.J. (1999). Small molecule inhibitor of mitotic spindle bipolarity identified in a phenotype-based screen. Science *286*, 971-974.

Meyer, H.H. (2005). Golgi reassembly after mitosis: the AAA family meets the ubiquitin family. Biochimica et biophysica acta *1744*, 108-119.

Meyer, H.H., Wang, Y., and Warren, G. (2002). Direct binding of ubiquitin conjugates by the mammalian p97 adaptor complexes, p47 and Ufd1-Npl4. EMBO J *21*, 5645-5652.

Misteli, T., and Warren, G. (1995). A role for tubular networks and a COP I-independent pathway in the mitotic fragmentation of Golgi stacks in a cell-free system. J Cell Biol *130*, 1027-1039.

Moore, M.J. (1975). Removal of glass coverslips from cultures flat embedded in epoxy resins using hydrofluoric acid. J Microsc *104*, 205-207.

Muller, J.M., Rabouille, C., Newman, R., Shorter, J., Freemont, P., Schiavo, G., Warren, G., and Shima, D.T. (1999). An NSF function distinct from ATPase-dependent SNARE disassembly is essential for Golgi membrane fusion. Nat Cell Biol *1*, 335-340.

Murray, A.W., and Szostak, J.W. (1985). Chromosome segregation in mitosis and meiosis. Annu Rev Cell Biol *1*, 289-315.

Nakajima, H., Yonemura, S., Murata, M., Nakamura, N., Piwnica-Worms, H., and Nishida, E. (2008). Myt1 protein kinase is essential for Golgi and ER assembly during mitotic exit. J Cell Biol *181*, 89-103.

Nardini, M., Spano, S., Cericola, C., Pesce, A., Massaro, A., Millo, E., Luini, A., Corda, D., and Bolognesi, M. (2003). CtBP/BARS: a dual-function protein involved in transcription co-repression and Golgi membrane fission. EMBO J *22*, 3122-3130.

Nebenfuhr, A., Frohlick, J.A., and Staehelin, L.A. (2000). Redistribution of Golgi stacks and other organelles during mitosis and cytokinesis in plant cells. Plant Physiol *124*, 135-151.

Niiya, F., Xie, X., Lee, K.S., Inoue, H., and Miki, T. (2005). Inhibition of cyclin-dependent kinase 1 induces cytokinesis without chromosome segregation in an ECT2 and MgcRacGAP-dependent manner. J Biol Chem *280*, 36502-36509.

Pecot, M.Y., and Malhotra, V. (2004). Golgi membranes remain segregated from the endoplasmic reticulum during mitosis in mammalian cells. Cell *116*, 99-107.

Pelletier, L., Jokitalo, E., and Warren, G. (2000). The effect of Golgi depletion on exocytic transport. Nat Cell Biol *2*, 840-846.

Pelletier, L., Stern, C.A., Pypaert, M., Sheff, D., Ngo, H.M., Roper, N., He, C.Y., Hu, K., Toomre, D., Coppens, I.*, et al.* (2002). Golgi biogenesis in Toxoplasma gondii. Nature *418*, 548-552.

Piel, M., Nordberg, J., Euteneuer, U., and Bornens, M. (2001). Centrosome-dependent exit of cytokinesis in animal cells. Science *291*, 1550-1553.

Preisinger, C., Korner, R., Wind, M., Lehmann, W.D., Kopajtich, R., and Barr, F.A. (2005). Plk1 docking to GRASP65 phosphorylated by Cdk1 suggests a mechanism for Golgi checkpoint signalling. EMBO J *24*, 753-765.

Preisinger, C., Short, B., De Corte, V., Bruyneel, E., Haas, A., Kopajtich, R., Gettemans, J., and Barr, F.A. (2004). YSK1 is activated by the Golgi matrix protein GM130 and plays a role in cell migration through its substrate 14-3-3zeta. J Cell Biol *164*, 1009-1020.

Preuss, D., Mulholland, J., Franzusoff, A., Segev, N., and Botstein, D. (1992). Characterization of the Saccharomyces Golgi complex through the cell cycle by immunoelectron microscopy. Mol Biol Cell *3*, 789-803.

Puthenveedu, M.A., Bachert, C., Puri, S., Lanni, F., and Linstedt, A.D. (2006). GM130 and GRASP65-dependent lateral cisternal fusion allows uniform Golgi-enzyme distribution. Nat Cell Biol *8*, 238-248.

Rabouille, C., Kondo, H., Newman, R., Hui, N., Freemont, P., and Warren, G. (1998). Syntaxin 5 is a common component of the NSF- and p97-mediated reassembly pathways of Golgi cisternae from mitotic Golgi fragments in vitro. Cell *92*, 603-610.

Rabouille, C., and Kondylis, V. (2007). Golgi ribbon unlinking: an organelle-based G2/M checkpoint. Cell cycle (Georgetown, Tex *6*, 2723-2729.

Rabouille, C., Levine, T.P., Peters, J.M., and Warren, G. (1995a). An NSF-like ATPase, p97, and NSF mediate cisternal regrowth from mitotic Golgi fragments. Cell *82*, 905-914.

Rabouille, C., Misteli, T., Watson, R., and Warren, G. (1995b). Reassembly of Golgi stacks from mitotic Golgi fragments in a cell-free system. J Cell Biol *129*, 605-618.

Reynolds, E.S. (1963). The use of lead citrate at high pH as an electron-opaque stain in electron microscopy. J Cell Biol *17*, 208-212.

Riggs, B., Rothwell, W., Mische, S., Hickson, G.R., Matheson, J., Hays, T.S., Gould, G.W., and Sullivan, W. (2003). Actin cytoskeleton remodeling during early Drosophila furrow formation requires recycling endosomal components Nuclear-fallout and Rab11. J Cell Biol *163*, 143-154.

Seemann, J., Pypaert, M., Taguchi, T., Malsam, J., and Warren, G. (2002). Partitioning of the matrix fraction of the Golgi apparatus during mitosis in animal cells. Science *295*, 848-851.

Shaul, Y.D., and Seger, R. (2006). ERK1c regulates Golgi fragmentation during mitosis. J Cell Biol *172*, 885-897.

Sheff, D., Pelletier, L., O'Connell, C.B., Warren, G., and Mellman, I. (2002). Transferrin receptor recycling in the absence of perinuclear recycling endosomes. J Cell Biol *156*, 797-804.

Shima, D.T., Cabrera-Poch, N., Pepperkok, R., and Warren, G. (1998). An ordered inheritance strategy for the Golgi apparatus: visualization of mitotic disassembly reveals a role for the mitotic spindle. J Cell Biol *141*, 955-966.

Shima, D.T., Haldar, K., Pepperkok, R., Watson, R., and Warren, G. (1997). Partitioning of the Golgi apparatus during mitosis in living HeLa cells. J Cell Biol *137*, 1211-1228.

Shinohara, M., Mikhailov, A.V., Aguirre-Ghiso, J.A., and Rieder, C.L. (2006). Extracellular signal-regulated kinase 1/2 activity is not required in mammalian cells during late G2 for timely entry into or exit from mitosis. Mol Biol Cell *17*, 5227-5240.

Shorter, J., Beard, M.B., Seemann, J., Dirac-Svejstrup, A.B., and Warren, G. (2002). Sequential tethering of Golgins and catalysis of SNAREpin assembly by the vesicle-tethering protein p115. J Cell Biol *157*, 45-62.

Shorter, J., and Warren, G. (1999). A role for the vesicle tethering protein, p115, in the post-mitotic stacking of reassembling Golgi cisternae in a cell-free system. J Cell Biol *146*, 57-70.

Shorter, J., and Warren, G. (2002). Golgi architecture and inheritance. Annu Rev Cell Dev Biol *18*, 379-420.

Shorter, J., Watson, R., Giannakou, M.E., Clarke, M., Warren, G., and Barr, F.A. (1999). GRASP55, a second mammalian GRASP protein involved in the stacking of Golgi cisternae in a cell-free system. EMBO J *18*, 4949-4960.

Sisson, J.C., Field, C., Ventura, R., Royou, A., and Sullivan, W. (2000). Lava lamp, a novel peripheral golgi protein, is required for Drosophila melanogaster cellularization. J Cell Biol *151*, 905-918.

Skop, A.R., Bergmann, D., Mohler, W.A., and White, J.G. (2001). Completion of cytokinesis in C. elegans requires a brefeldin A-sensitive membrane accumulation at the cleavage furrow apex. Curr Biol *11*, 735-746.

Skoufias, D.A., Debonis, S., Saoudi, Y., Lebeau, L., Crevel, I., Cross, R., Wade, R.H., Hackney, D., and Kozielski, F. (2006). S-trityl-l-cysteine is a reversible, tight-binding inhibitor of the human kinesin Eg5 that specifically blocks mitotic progression. J Biol Chem *281*, 17559-17569.

Sonnichsen, B., Lowe, M., Levine, T., Jamsa, E., Dirac-Svejstrup, B., and Warren, G. (1998). A role for giantin in docking COPI vesicles to Golgi membranes. J Cell Biol *140*, 1013-1021.

Stinchcombe, J.C., Majorovits, E., Bossi, G., Fuller, S., and Griffiths, G.M. (2006). Centrosome polarization delivers secretory granules to the immunological synapse. Nature *443*, 462-465.

Storrie, B., White, J., Rottger, S., Stelzer, E.H., Suganuma, T., and Nilsson, T. (1998). Recycling of golgi-resident glycosyltransferases through the ER reveals a novel pathway and provides an explanation for nocodazole-induced Golgi scattering. J Cell Biol *143*, 1505-1521.

Stout, J.R., Rizk, R.S., Kline, S.L., and Walczak, C.E. (2006). Deciphering protein function during mitosis in PtK cells using RNAi. BMC Cell Biol *7*, 26.

Sutterlin, C., Hsu, P., Mallabiabarrena, A., and Malhotra, V. (2002). Fragmentation and dispersal of the pericentriolar Golgi complex is required for entry into mitosis in mammalian cells. Cell *109*, 359-369.

Tang, D., Mar, K., Warren, G., and Wang, Y. (2008). Molecular mechanism of mitotic Golgi disassembly and reassembly revealed by a defined reconstitution assay. J Biol Chem *283*, 6085-6094.

Tyson, J.J., and Novak, B. (2008). Temporal organization of the cell cycle. Curr Biol *18*, R759-R768.

Uchiyama, K., Jokitalo, E., Lindman, M., Jackman, M., Kano, F., Murata, M., Zhang, X., and Kondo, H. (2003). The localization and phosphorylation of p47 are important for Golgi disassembly-assembly during the cell cycle. J Cell Biol *161*, 1067-1079.

Uchiyama, K., Totsukawa, G., Puhka, M., Kaneko, Y., Jokitalo, E., Dreveny, I., Beuron, F., Zhang, X., Freemont, P., and Kondo, H. (2006). p37 is a p97 adaptor required for Golgi and ER biogenesis in interphase and at the end of mitosis. Developmental cell *11*, 803-816.

van Rijnsoever, C., Oorschot, V., and Klumperman, J. (2008). Correlative light-electron microscopy (CLEM) combining live-cell imaging and immunolabeling of ultrathin cryosections. Nat Methods *5*, 973-980.

Wang, L., Wang, Z.B., Zhang, X., FitzHarris, G., Baltz, J.M., Sun, Q.Y., and Liu, X.J. (2008a). Brefeldin A disrupts asymmetric spindle positioning in mouse oocytes. Dev Biol *313*, 155-166.

Wang, Y., Satoh, A., Warren, G., and Meyer, H.H. (2004). VCIP135 acts as a deubiquitinating enzyme during p97-p47-mediated reassembly of mitotic Golgi fragments. J Cell Biol *164*, 973-978.

Wang, Y., Seemann, J., Pypaert, M., Shorter, J., and Warren, G. (2003). A direct role for GRASP65 as a mitotically regulated Golgi stacking factor. EMBO J *22*, 3279-3290.

Wang, Y., Wei, J.H., Bisel, B., Tang, D., and Seemann, J. (2008b). Golgi Cisternal Unstacking Stimulates COPI Vesicle Budding and Protein Transport. PLoS ONE *3*, e1647.

Warren, G. (1993). Membrane partitioning during cell division. Annu Rev Biochem *62*, 323-348.

Warren, G., and Wickner, W. (1996). Organelle inheritance. Cell *84*, 395-400.

Wei, J.H., and Seemann, J. (2009). The mitotic spindle mediates inheritance of the Golgi ribbon structure. J Cell Biol *184*, 391-397.

Xiang, Y., Seemann, J., Bisel, B., Punthambaker, S., and Wang, Y. (2007). Active ADP-ribosylation factor-1 (ARF1) is required for mitotic Golgi fragmentation. J Biol Chem *282*, 21829-21837.

Xie, S., Wang, Q., Ruan, Q., Liu, T., Jhanwar-Uniyal, M., Guan, K., and Dai, W. (2004). MEK1-induced Golgi dynamics during cell cycle progression is partly mediated by Polo-like kinase-3. Oncogene *23*, 3822-3829.

Xu, H., Brill, J.A., Hsien, J., McBride, R., Boulianne, G.L., and Trimble, W.S. (2002). Syntaxin 5 is required for cytokinesis and spermatid differentiation in Drosophila. Dev Biol *251*, 294-306.

Yadav, S., Puri, S., and Linstedt, A.D. (2009). A Primary Role for Golgi Positioning in Directed Secretion, Cell Polarity and Wound Healing. Mol Biol Cell.

Yang, L., Guan, T., and Gerace, L. (1997). Integral membrane proteins of the nuclear envelope are dispersed throughout the endoplasmic reticulum during mitosis. J Cell Biol *137*, 1199-1210.

Yoshimura, S., Yoshioka, K., Barr, F.A., Lowe, M., Nakayama, K., Ohkuma, S., and Nakamura, N. (2005). Convergence of cell cycle regulation and growth factor signals on GRASP65. J Biol Chem *280*, 23048-23056.

Zaal, K.J., Smith, C.L., Polishchuk, R.S., Altan, N., Cole, N.B., Ellenberg, J., Hirschberg, K., Presley, J.F., Roberts, T.H., Siggia, E.*, et al.* (1999). Golgi membranes are absorbed into and reemerge from the ER during mitosis. Cell *99*, 589-601.

Zhou, Y., Atkins, J.B., Rompani, S.B., Bancescu, D.L., Petersen, P.H., Tang, H., Zou, K., Stewart, S.B., and Zhong, W. (2007). The mammalian Golgi regulates numb signaling in asymmetric cell division by releasing ACBD3 during mitosis. Cell *129*, 163-178.